

# Symbolic Constraints in Polyhedral Enclosure and Tetrahedral Decomposition in Genus-0 Polyhedra

Moustapha Itani

ORCID: 0000-0001-9372-3715

*Email:* `moustapha.itani@helsinki.fi`

December 29, 2025

## Abstract

I present a coordinate-free, symbolic framework for determining whether a given set of polygonal faces can form a closed, genus-zero polyhedral surface and for predicting admissible internal tetrahedral decompositions consistent with incidence constraints. The method uses only discrete combinatorial variables, such as the number of tetrahedra  $T$ , internal gluing triangles  $N_i$ , and internal triangulation segments  $S_i$ , and applies feasibility checks prior to any geometric embedding.

For polyhedra in *normal form*, I record exact incidence identities linking  $V$ ,  $E$ , and  $F$  to a flatness parameter  $S := \sum_f (\deg f - 3)$ , and identify parity-sensitive extremal behavior in  $E$ ,  $F$ , and  $S$  arising from minimal vertex-degree constraints. These external identities and parity-dependent bounds hold for genus-zero polyhedral graphs under standard simplicity and connectivity assumptions. For internal quantities, I prove exact relations  $N_i = 2T - V + 2$  and  $T - N_i + S_i = 1$ , and derive restricted linear ranges for tetrahedral decompositions in normal form with no interior vertices. Together, these results yield a symbolic workflow for rapid pre-screening of combinatorially impossible configurations, reducing reliance on costly geometric validation in computational geometry, graphics, and automated modeling. An open-source R implementation is available at <https://github.com/MoustaphaItani/polyenclose/>.

## Tagging of Results:

- **Proposition / Lemma:** Proved in this paper or from established literature in genus-zero polyhedra in normal form.
- **Conjectural Proposition:** Believed true, supported by examples, but no general proof.
- **Heuristic Proposition:** Empirical or pattern-based rule, not formally proved.
- **Observation:** Fact specific to worked examples, not claimed to hold generally.

**Author’s Note:** This document represents original, exploratory research conducted independently by the author. It does not reflect the views or positions of any affiliated institution. The author does not claim to be a professional mathematician and welcomes constructive feedback, critical review, and potential collaboration to refine or expand upon the ideas presented.

## 1 Introduction and Background

This paper introduces a purely combinatorial framework for assessing the feasibility of polyhedral enclosures in three-dimensional space, based solely on symbolic logic and integer arithmetic. Unlike traditional geometric methods that rely on coordinates, angles, or embeddings, this approach evaluates the structural validity of polygonal configurations through discrete operations such as triangulation segment counts, vertex valency rules, and symbolic angle units.

**Scope and fixed assumptions:** Throughout this work, I limit attention to *genus-zero (simply connected) surfaces*, with no geometric embeddability tests (i.e., no attempt to prove realizability in  $\mathbb{R}^3$ ), and

without consideration of higher-genus or non-manifold topologies. Unless stated otherwise, all internal “range” results are given under the strict internal decomposition procedure described in the Methods section, i.e. normal form with at most one new interior segment per layer, introduced only when necessary. All identities and bounds presented are *symbolic rather than metric*, and some are conjectural or supported by empirical validation rather than proved in full generality.

This work is exploratory and intended as a conceptual and symbolic approach to studying polyhedral closure. The methodology emerged from empirical analysis of polyhedral forms and was later formalized with computational assistance. It seeks to answer a longstanding question: when can a set of polygons form a valid 3D enclosure, and how can such enclosures be systematically analyzed or decomposed without geometric tools?

The approach is related in spirit to Ziegler’s symbolic treatment of polytopes [10] and to combinatorial efforts in tetrahedral decomposition (e.g., [4]), but differs in its exclusive reliance on integer logic and symbolic topological consistency. A classical result by Steinitz [8] shows that a graph is the 1-skeleton of a convex 3-polyhedron if and only if it is planar and 3-connected, providing the foundational combinatorial criterion for convex polyhedral graphs. While many known polyhedral validation tools rely on coordinate-based embeddings or optimization algorithms, the framework presented here derives topological invariants and structural bounds without any reference to spatial realization.

Recent extensions of Steinitz’s theorem have been explored for ball polyhedra [1], and Gallier and Quaintance [5] provide a contemporary combinatorial-topological survey covering shellings, Euler–Poincaré relationships, and triangulations. From a computational perspective, Below, De Loera, and Richter-Gebert [3] proved that finding a triangulation with the minimum number of tetrahedra is NP-complete. In contrast, the present method uses empirical observations to guide symbolic enumeration and narrow down the space of combinatorial configurations that may support enclosure and decomposition.

**New contributions.** For genus-zero polyhedral graphs in normal form, I record exact external identities linking  $(V, E, F)$  to the face-degree excess (flatness)

$$S := \sum_f (\deg f - 3),$$

namely

$$E = 3V - 6 - S, \quad F = 2V - 4 - S,$$

proved in Proposition 4.1. Combining these with the minimum degree condition  $\deg(v) \geq 3$  yields parity-sensitive extremal bounds on  $E$ ,  $F$ , and  $S$  (Lemma 4.1 and Corollary 4.2).

The resulting extremal ranges are summarized in Corollary 4.2.

*Remark.* For even  $V$ , equality in Lemma 4.1 is achieved by cubic (polyhedral) graphs such as prisms, the cube, and the dodecahedron. For odd  $V$ , equality requires exactly one 4-valent vertex and all others trivalent; explicit realizations exist for many  $V$ , though no classification is claimed here.

Building on this, I propose an *extended Euler-type heuristic*:

$$V - E + F = 2(T - N_i + S_i),$$

linking external incidence data to internal decomposition variables:  $T$  = internal tetrahedra,  $N_i$  = internal gluing triangles,  $S_i$  = internal triangulation segments.

This identity reduces to the classical Euler formula when  $T - N_i + S_i = 1$  (as in minimal or marching tetrahedralizations). Although not yet proved as a general necessity theorem, it functions as a strong symbolic consistency check.

Finally, empirical enumeration suggests a sharp rigidity phenomenon at the top of the internal ladder: *bipyramidal* (bipyramidal–prism) polyhedra appear to be the only normal-form surfaces attaining  $T_{\max}$ , and their internal invariants  $(T, N_i, S_i)$  are essentially *S-inflexible*, admitting no variation in the external parameters  $(E, F, S)$  that is compatible with a valid tetrahedral decomposition. More generally, determining how the realized set of admissible triples  $(T, N_i, S_i)$  *contracts* as the surface flatness  $S$  increases remains open, and may admit either an empirical resolution via systematic enumeration or a theoretical one.

This document is structured as both a **conceptual foundation** and a **practical toolbox** for symbolic polyhedral reasoning. The core objective is to determine when a collection of polygonal faces, without any geometric embedding, can enclose a valid 3D volume, and if so, what internal structure it might support.

To ensure clarity, **Table 1 summarizes the key variables and symbolic terms** used throughout this document. These variables describe either the external surface of a polyhedron or structures required for its internal decomposition into tetrahedra.

Symbol	Meaning
<i>Surface / External Structure Variables</i>	
$V$	Number of vertices
$E$	Number of edges
$F$	Number of faces
$S$	External non-intersecting triangulation segments (used to triangulate surface); also used throughout as a discrete flatness measure
$N$	Total internal angle units on the external surface (1 unit = $\pi$ radians = $180^\circ$ )
$F_\Delta$	Number of boundary triangular faces resulting from the triangulation of the entire polyhedral surface
$M$	External angle fullness units (derived from polygon types)
$F_3, F_4, F_5, \dots$	Face types: triangle (3 sides), quadrilateral (4), pentagon (5), etc.
$V_3, V_4, V_5, \dots$	Vertex types: valency 3 (3 incident edges), valency 4, valency 5, etc.
<i>Internal Decomposition Variables</i>	
$T$	Number of internal tetrahedra (used to fill the volume)
$N_i$	Number of internal gluing angle units (each unit = one triangle)
$S_i$	Number of interior edges (internal non-intersecting triangulation segments). In normal form there are no interior vertices, hence $S_i \equiv E_i$
$E_i$	(Alias) Number of interior edges; in normal form $E_i = S_i$
$V_i$	Internal vertices

Table 1: Key variables used in the symbolic framework. *Surface/external* variables describe the boundary structure, while *internal* variables capture the combinatorial scaffolding of tetrahedral decompositions. This grouping highlights the two structural layers that the framework relates through symbolic identities.

The variables above are not derived from physical measurements or coordinates, but from symbolic relationships among discrete structural components. For example, angle units are treated symbolically as multiples of  $\pi$ , and surface structures are quantified via segment and gluing unit counts rather than metric angles or lengths.

The auxiliary variables  $N$ ,  $M$ ,  $S$ ,  $N_i$ , and  $S_i$  do not appear in the classical Euler–Steinitz framework. They are introduced here to support symbolic decomposition bookkeeping and to connect surface composition to volumetric tetrahedralization.  $N$  represents the total internal angle units on the external surface, with one unit defined as  $= \pi$  radians ( $= 180^\circ$ ).  $M$  is derived from polygon types and measures “external angle fullness” in the same units.  $S$  counts the non-intersecting triangulation segments added to polygonal faces to produce a fully triangulated surface and also serves as a discrete flatness measure.  $N_i$  counts the number of internal gluing angle units, each corresponding to a shared triangular face between two tetrahedra.  $S_i$  counts the internal non-intersecting triangulation segments required to complete a volumetric mesh during decomposition. None of these auxiliary quantities are edges in the polyhedron’s graph; they exist only in the symbolic model and may not correspond to realizable geometric features.

### 1.1 Illustrative Examples of $N_i$ , $S$ , and $S_i$

**Rectangular Pyramid ( $S = 1$ ):** A five-vertex polyhedron with a quadrilateral base and one apex point. To triangulate the external surface, a single diagonal segment divides the base into two triangles, yielding  $S = 1$ .

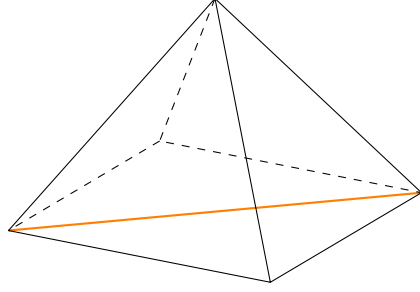


Figure 1: Rectangular pyramid illustrating the flatness measure  $S$ . The single internal diagonal on the quadrilateral base (orange) is the unique surface triangulation segment needed to obtain a fully triangulated boundary, hence  $S = 1$ . This corresponds to one coplanarity merge relative to the maximally triangulated case and, by Proposition 4.2, decreases both  $F$  and  $E$  by 1 while preserving  $V$  and  $\chi = 2$ .

**Triangular Bipyramid ( $N_i = 1$ ):** Composed of two tetrahedra joined along a shared triangular face, this structure has one gluing triangle (blue):  $N_i = 1$ .

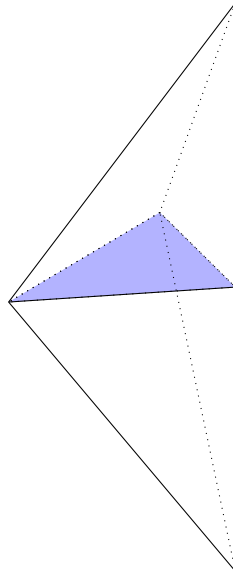


Figure 2: Triangular bipyramid obtained by gluing two tetrahedra along a common triangular face (highlighted in blue). This shared face corresponds to exactly one internal gluing triangle, hence  $N_i = 1$  in the symbolic model. It provides the simplest example of how  $N_i$  is counted: each such internal face removes two boundary triangles in the fully triangulated representation, linking interior adjacency directly to external face counts via Proposition 5.4.

**Irregular Octahedron ( $S_i = E_i = 1$ ,  $N_i = 4$ ):** When regular, constructed by gluing two rectangular pyramids base-to-base. In the case of this irregular octahedron, the internal meshwork between the glued tetrahedra must be constructed by adding one internal segment functioning as an internal edge, yielding  $S_i = E_i = 1$ . Once included, four gluing triangles would emerge, resulting in  $N_i = 4$ .

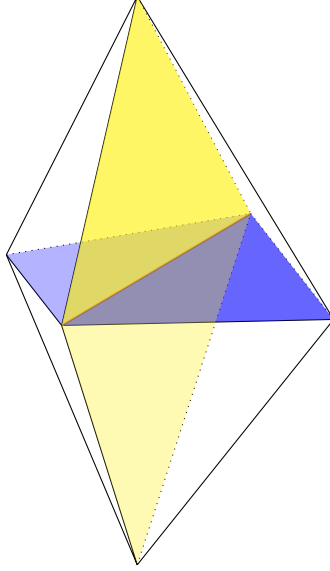


Figure 3: Irregular octahedron constructed by gluing two quadrilateral-based pyramids along their bases. The orange segment is an internal triangulation segment ( $S_i = 1$ ) required to fully mesh the internal volume into tetrahedra without adding new vertices. This configuration produces four internal gluing triangles ( $N_i = 4$ ), shown in blue and yellow, illustrating how  $S_i$  and  $N_i$  together describe the combinatorial scaffolding of the internal decomposition.

## 2 Preliminaries

### 2.1 Normal form and standing assumptions

**Definition 2.1** (Normal form). A genus-0 polyhedron is in normal form if: (i) all vertices lie on the boundary (no interior/Steiner vertices, so  $V_i \equiv 0$ ); (ii) edges are straight segments that intersect only at shared endpoints (boundary 1-skeleton is a planar straight-line graph); (iii) every interior edge is an internal triangulation segment between boundary vertices and is incident to exactly two distinct triangular faces; and (iv) internal adjacencies occur only along triangular faces (no edge bisections).

*Remark* (Notation and scope). Throughout,  $S := \sum_f (\deg f - 3)$  denotes flatness. Unless stated otherwise, all identities tagged “Proposition” are proved under normal form; anything tagged “Heuristic” or “Conjectural Proposition” is indicated where used.

## 3 Methods and Heuristics

This section introduces both the *proved combinatorial identities* and the *empirical heuristics* that underlie the framework, along with the triangulation logic that directs it towards constructing a polyhedron’s internal mesh.

### 3.1 Logical separation of results

Two classes of structural constraints are used in this work:

1. **Proved genus-zero identities:** These are exact, rigorously derived equalities and bounds that hold for all genus-zero polyhedra in *normal form*. Chief among the proved results is the flatness identity

$$E = 3V - 6 - S, \quad F = 2V - 4 - S,$$

where  $S := \sum_f (\deg f - 3)$  (Proposition 4.1). Combining this with the minimum degree condition  $\deg(v) \geq 3$  yields parity-sensitive extremal bounds on  $E$ ,  $F$ , and  $S$  (Lemma 4.1 and Corollary 4.2).

2. **Empirical and conjectural constraints:** These are patterns and formulas suggested by extensive manual and computational enumeration but not proved in general. A key example is the extended Euler-type identity

$$V - E + F = 2(T - N_i + S_i),$$

where  $T$  is the number of internal tetrahedra,  $N_i$  is the number of internal gluing triangles, and  $S_i$  is the number of internal triangulation segments. This identity is *proved* for certain construction sequences but remains a *conjectural proposition* in full generality.

In what follows, the derivation of heuristic bounds and decomposition strategies is always annotated with the appropriate tag (*Heuristic*, *Proposition*, or *Conjectural proposition*).

### 3.2 Empirical observation and validation

Through iterative experimentation, I tracked the effects of adding or removing one structural element at a time. On the surface, I examined vertices, edges, faces, and triangulation segments; internally, I observed how tetrahedra filled the polyhedron and how their gluing faces were defined by internal triangulation segments. I recorded all countable variables and analyzed their relationships. These empirical observations guided both the decomposition strategy and the derivation of formulas describing how both external and internal structures scale with vertex count and triangulation complexity (i.e., surface flatness). Extremal values of these variables were described as functions of  $V$ , and sequences were defined to characterize how they change relative to one another with increasing flatness for fixed  $V$ .

### 3.3 Surface flatness estimation

To quantify *flatness* on the surface, I use the face-degree excess

$$S := \sum_f (\deg f - 3),$$

which equals the total number of non-intersecting diagonals needed to triangulate all polygonal faces. Thus  $S = 0$  if and only if every face is triangular, and increasing  $S$  corresponds to fewer faces and edges relative to the triangulated case via Proposition 4.1.

*Remark.* Because the embedding is planar with all faces homeomorphic to disks (i.e., a 2-cell embedding of  $S^2$ ), each edge is incident to exactly two distinct faces.

Each polygonal face is triangulated by drawing non-intersecting segments between the nearest connectable vertices. The cumulative count of these added segments on all external faces constitutes the flatness measure  $S$ . When all faces of a polyhedron are triangles,  $S = 0$  and  $F \equiv F_{\text{ub}}$ .

### 3.4 Internal mesh construction from surface triangulation

Unlike the external surface of a polyhedron, which is both observable and abstractable with consistency, the internal structure must be inferred. Consequently, the number of tetrahedra required to tetrahedralize a polyhedron, such as a cube, depends critically on the configuration of face cuts. For example, as noted by Timalsina and Knepley [9], a cube may be divided into 5, 6, or 12 tetrahedra depending on the chosen strategy: five tetrahedra in an ideal face-aligned configuration, six using the marching tetrahedra algorithm, and twelve when a Steiner point is introduced at the cube’s center.

Since the goal of this exploration is to maximally preserve the original topology of the polyhedron, I adopt a triangulated, face-aligned tetrahedralization strategy. For this purpose, the internal mesh is constructed solely from external constraints, namely, the original vertices and triangulated faces.

To support this construction, internal triangulation segments are introduced to define the internal gluing triangles along which tetrahedra are joined. Each internal segment contributes once to the structural count  $S_i$ , and each internal triangle used for gluing contributes once to the structural count  $N_i$ , regardless of how many tetrahedra share them. Together, these inferred internal edges and triangle faces form a combinatorial scaffold that enables complete internal tetrahedralization while preserving the external surface geometry.

### 3.5 Normal-form restrictions on interior structure

Restricting attention to *normal form* constructions: all vertices lie on the boundary of the enclosing polygonal face, and no two edges intersect except at shared endpoints. In particular, interior vertices  $V_i$  (vertices not incident to the boundary) cannot arise under these constraints, so  $V_i \equiv 0$  in all cases considered. Moreover, every interior edge  $E_i$  is necessarily an internal triangulation segment  $S_i$ , each belonging to exactly two distinct triangular faces. These conditions ensure that the triangulation is a planar straight-line graph in the classical sense, with all internal segments disjoint except at endpoints.

### 3.6 Tetrahedral decomposition and trivalent vertex prioritization

Original edges, surface triangulation segments, internal gluing triangles, and internal triangulation segments constitute the structure necessary to decompose the polyhedron into tetrahedra. These tetrahedra are joined along fully triangulated internal faces and, unless fully embedded, are partially or fully coned outward toward external triangulated faces. The coning of fully embedded tetrahedra is progressively revealed as the surrounding shell of tetrahedra is “chipped away” one at a time.

Tetrahedra are incrementally removed by eliminating vertices. Priority is given to trivalent vertices, those connected to exactly three edges, since each such vertex typically defines a single tetrahedron when coned to its surrounding triangular link. This targeted removal minimizes combinatorial complexity, which can occur when higher-valency vertices are eliminated without the right internal triangulation, potentially leading to more complex subdivisions and increased tetrahedral counts. When it is necessary to remove more complex vertices or parts of the polyhedron, the separation must occur across a single plane dividing coplanar vertices. Failing to respect such planar separations can result in the bisection of edges and faces, thereby increasing internal complexity.

This approach differs from geometric decompositions which rely on slicing through faces or bisecting edges to create tetrahedral meshes. In contrast, the method presented here preserves polygonal integrity: despite triangulation, all faces remain whole, with fixed vertex sets. No edge bisection is allowed and no midpoint or interior vertex insertion (Steiner points) is permitted. As internal tetrahedra are constructed exclusively through explicit gluing at existing vertices, internal adjacencies occur only along triangular faces.

This work restricts attention to genus-0, normal-form decompositions built by peeling one outer shell of tetrahedra at a time, a procedure I will refer to informally as a *shell-aligned ladder tetrahedralization* (SALT). Each layer is created by coning existing boundary triangles. Within this scheme, a “minimal interior edge” (MIE) rule is observed: a new interior segment between boundary vertices is introduced only when strictly necessary to complete the current triangular gluing layer; otherwise, none is added. This SALT+MIE restriction excludes dense interior diagonals between boundary vertices (e.g. pulling triangulations of cyclic polytopes), which can create  $\Theta(V^2)$  tetrahedra without adding vertices.

### 3.7 Validations of observed relations by Euler’s characteristic

Euler’s characteristic is used here to validate the internal consistency of the framework.

The first validation is purely surface-based and corresponds to *Proposition 4.1* together with *Corollary 4.2*. Beginning from the classical Euler characteristic and, in the genus-zero case, using incidence counting, I derive the proved flatness identity

$$E = 3V - 6 - S, \quad F = 2V - 4 - S,$$

together with its associated extremal bounds. This establishes the exact relationship between  $V$ ,  $E$ ,  $F$ , and  $S$  for genus-zero polyhedra in normal form.

The second validation links surface quantities to internal decomposition variables. Using *Proposition 5.4*, which expresses the boundary counts in terms of  $T$  (internal tetrahedra),  $N_i$  (internal gluing triangles), and  $S_i$  (internal triangulation segments), I obtain the extended Euler-type heuristic

$$V - E + F = 2(T - N_i + S_i).$$

This reduces to the classical value  $\chi = 2$  because  $T - N_i + S_i = 1$  along that ladder. Outside those sequences the identity is treated as a conjectural proposition pending a general proof.

### 3.8 Results taxonomy

Throughout the paper, statements are tagged as *Heuristic*, *Proposition*, or *Conjectural proposition*. *Heuristic* marks empirically validated bounds or patterns supported by computations and worked examples but not proved in full generality. *Proposition* denotes identities for which a complete proof is provided under stated hypotheses. *Conjectural proposition* designates candidate general identities whose proof would require showing that certain construction sequences cover all admissible decompositions.

## 4 Vertex-Driven External Polyhedral Properties: Intermediate Flatness Realizability and Parity Effects

I establish extremal bounds on external combinatorial quantities ( $F$ ,  $E$ , and  $S$ ) directly as functions of the vertex count  $V$ . These bounds emerge from Euler’s characteristic combined with flatness-based adjustments, and serve as the foundation for linking external structure to the internal decomposition results in later sections. This section establishes the admissible parity-sensitive bounds on  $E$ ,  $F$ , and  $S$  and presents heuristic evidence that every integer flatness value  $0 \leq S \leq S_{\text{ub}}$  is realizable by some genus-zero polyhedron in normal form. The realizability result is stated formally in *Proposition 4.3*.

The derivation proceeds from a given number of vertices  $V \in \mathbb{N}$ , showing how faces, edges, and triangulation segments co-evolve under Euler-consistent constraints. I examine parity effects in the incidence structure. Although Euler’s characteristic  $\chi = V - E + F$  is invariant under vertex-parity changes, quantities such as  $E$ ,  $F$ , and  $S$  can vary systematically between even and odd  $V$ . These parity-sensitive patterns have implications for both surface enumeration and internal tetrahedral decomposition strategies. From this, I obtain a feasible range of structural properties for a closed 3D polyhedron and assess their validity using Euler’s formula.

### 4.1 Vertex Basis and Initial Angle Unit Calculation

Let  $V \geq 4$  be the number of vertices in the polyhedron. I define:

- $N$ : the total number of angle units on the external surface, where **one unit** =  $180^\circ$ , i.e., the internal angle of a triangle.
- I assume full triangulation of the surface, where polygonal faces are split into triangles using non-intersecting internal segments through alternating vertices.

Then the total number of surface angle units is:

$$N = 2(V - 2).$$

*Remark* (Triangulated baseline and flattening intuition). When the boundary is fully triangulated (i.e.  $S = 0$ ), one has  $F_{\text{ub}} = 2V - 4$  and  $E_{\text{ub}} = 3V - 6$ . Interpreting  $S = \sum_f (\deg f - 3)$  as the total triangulation deficit, each unit increase of  $S$  corresponds to removing one diagonal from a triangulated refinement, decreasing both  $E$  and  $F$  by one. The formal identities are stated and proved in Proposition 4.1.

**Proposition 4.1** (External structure formulas). *For a genus-0 polyhedral graph in normal form with  $V$  vertices,  $E$  edges,  $F$  faces, and face-degree excess*

$$S := \sum_f (\deg f - 3),$$

*the following identities hold:*

$$E = 3V - 6 - S, \quad F = 2V - 4 - S.$$

*Proof.* Because the embedding is a 2-cell embedding of  $S^2$ , each edge is incident to exactly two faces, hence  $\sum_f \deg f = 2E$ . By definition,  $S = \sum_f (\deg f - 3) = 2E - 3F$ . Euler's formula gives  $F = E - V + 2$ . Substituting,

$$S = 2E - 3(E - V + 2) = 3V - 6 - E,$$

so  $E = 3V - 6 - S$ , and then  $F = E - V + 2 = 2V - 4 - S$ .

**Lemma 4.1** (Lower bound edges from trivalence). *Let  $G$  be the 1-skeleton of a genus-0 polyhedron (simple, planar, and 3-connected) with  $V \geq 4$  vertices and  $E$  edges. Then*

$$E \geq \left\lceil \frac{3V}{2} \right\rceil,$$

with equality when:

1.  $V$  is even and all vertices are trivalent (degree 3); or
2.  $V$  is odd and all but one vertex are trivalent, the remaining vertex being 4-valent.

*Proof.* Every vertex has degree at least 3, so by the handshake lemma

$$2E = \sum_{v \in V} \deg(v) \geq 3V,$$

which yields  $E \geq \lceil 3V/2 \rceil$ .

If  $V$  is even and all vertices have degree 3, then  $2E = 3V$  and  $E = 3V/2$ , attaining the bound.

If  $V$  is odd and all but one vertex are trivalent and the remaining vertex is 4-valent, then  $2E = 3(V - 1) + 4 = 3V + 1$ , so  $E = (3V + 1)/2$ , again attaining the bound.

In the symbolic flatness framework, both equality cases correspond to  $S = S_{\text{ub}}$  and  $F = F_{\text{lb}}$  (see Corollary 4.2).

**Corollary 4.1** (Parity restriction on the minimal edge count). *Let  $G$  be the 1-skeleton of a genus-0 polyhedron in normal form (simple, planar, 3-connected) with  $V$  vertices and  $E$  edges. If  $V$  is odd, then  $E \neq \frac{3V}{2}$  by integrality. Hence*

$$E_{\text{lb}} = \left\lceil \frac{3V}{2} \right\rceil = \frac{3V + 1}{2}.$$

*Remark.* For odd  $V$ , the degree multiset achieving  $E_{\text{lb}}$  necessarily has one 4-valent vertex and all others trivalent (by the handshake lemma). Realization for all odd  $V$  is a separate existence question; examples exist for many  $V$  (e.g., small explicit polyhedral graphs), but a full classification is beyond our scope.

**Corollary 4.2** (Relating maximal flatness and minimal faces). *For  $V \geq 4$ , let  $E_{\text{lb}} = \lceil 3V/2 \rceil$ . Then with the formulas from Proposition 4.1:*

$$S_{\text{ub}} = 3V - 6 - E_{\text{lb}} = \begin{cases} \frac{3V}{2} - 6, & V \text{ even,} \\ \frac{3V}{2} - \frac{13}{2}, & V \text{ odd,} \end{cases} \quad F_{\text{lb}} = 2 - V + E_{\text{lb}} = \begin{cases} \frac{V}{2} + 2, & V \text{ even,} \\ \frac{V}{2} + \frac{5}{2}, & V \text{ odd.} \end{cases}$$

Moreover, as  $S$  increases by 1 (flattening step), both  $E$  and  $F$  decrease by 1, and for  $k = 0, 1, \dots, S_{\text{ub}}$  one has  $E = 3V - 6 - k$ ,  $F = 2V - 4 - k$ .

*Remark. On parity and the ‘‘half’’ constants.* The halves (e.g.,  $S_{\text{ub}} = \frac{3V}{2} - \frac{13}{2}$  for odd  $V$ ) come from the integer lower bound  $E_{\text{lb}} = \lceil 3V/2 \rceil$ . Writing

$$S_{\text{ub}} = 3V - 6 - E_{\text{lb}}$$

gives  $S_{\text{ub}} = \frac{3V}{2} - 6$  when  $V$  is even and  $S_{\text{ub}} = \frac{3V}{2} - \frac{13}{2}$  when  $V$  is odd; these evaluate to integers at the respective parities. The corresponding formulas for  $F_{\text{lb}} = 2 - V + E_{\text{lb}}$  have the same source.

*Proof.* Substitute  $E_{\text{lb}}$  into the formulas in Proposition 4.1.

## 4.2 Triangulation Sequences and the Invariance of Euler’s Characteristic

This proposition is included only to formalize the triangulated baseline and the “flattening ladder” interpretation; the definitive identities are Proposition 4.1 and Corollary 4.2.

**Proposition 4.2** (Triangulated extrema and invariance of  $\chi$ ). *For a genus-zero polyhedral surface composed entirely of triangles,*

$$F_{\text{ub}} = 2(V - 2), \quad E_{\text{ub}} = 3(V - 2).$$

*If  $S$  denotes the number of coplanarity merges of adjacent triangles (each merge decreases both  $F$  and  $E$  by 1 while  $V$  is fixed), then for all  $S$  in the admissible range,*

$$F(S) = F_{\text{ub}} - S, \quad E(S) = E_{\text{ub}} - S, \quad V - E(S) + F(S) = 2.$$

*Proof.* Each triangle has three edges and each edge is shared by two triangles, so  $2E_{\text{ub}} = 3F_{\text{ub}}$ . Substituting  $E_{\text{ub}} = \frac{3}{2}F_{\text{ub}}$  into Euler’s formula  $V - E_{\text{ub}} + F_{\text{ub}} = 2$  yields  $F_{\text{ub}} = 2(V - 2)$  and  $E_{\text{ub}} = 3(V - 2)$ . A coplanarity merge of two adjacent triangles removes one surface edge and one triangle, so  $F \mapsto F - 1$  and  $E \mapsto E - 1$  with  $V$  unchanged. Hence  $V - E + F$  is invariant and equal to 2 for all admissible  $S$ .

**Equivalent parameterization for fixed  $V$  from the lower extremum.** Equivalently, indexing the flattening ladder from the lower extremal configuration  $(S_{\text{ub}}, E_{\text{lb}}, F_{\text{lb}})$ , one may write

$$S_k = S_{\text{ub}} - k, \quad E_k = E_{\text{lb}} + k, \quad F_k = F_{\text{lb}} + k,$$

for  $k = 0, 1, \dots, S_{\text{ub}}$ . This parameterization enumerates all admissible external configurations consistent with the flattening rule and Euler invariance.

This result shows that the maximal triangulated case ( $S = 0$ ) fixes  $F$  and  $E$  uniquely in terms of  $V$ , and that the Euler characteristic is preserved under a sequence of coplanarity merges parameterized by  $S$ . In our framework,  $S$  also functions as a discrete measure of flatness and appears in parity-sensitive bounds in this section, and will reappear in linking external and internal structures (§5). Appendix A lists worked examples for  $V = 4$  to  $V = 7$  illustrating these sequences and confirming  $V - E + F = 2$  in all cases.

**Heuristic Proposition 4.3** (Flatness values in the admissible range can be realized). *Fix  $V \geq 4$ . For every integer  $S$  with  $0 \leq S \leq \frac{3V}{2} - 6$  when  $V$  is even and  $0 \leq S \leq \frac{3V}{2} - \frac{13}{2}$  when  $V$  is odd, one can construct a genus-0 polyhedron in normal form (equivalently, a simple 3-connected planar graph) with*

$$E = 3V - 6 - S, \quad F = 2V - 4 - S.$$

*In particular, every integer flatness value in the admissible range is realized.*

*Proof sketch.* Start from any maximally planar (triangulated) 3-connected planar graph on  $V$  vertices (e.g., a stacked triangulation), which has  $S = 0$ ,  $E = 3V - 6$ ,  $F = 2V - 4$ . A “coplanarity merge” of two adjacent boundary triangles corresponds combinatorially to deleting their shared edge, which decreases both  $E$  and  $F$  by 1 and keeps  $V$  fixed. In a stacked triangulation one can choose a set of  $V - 4$  edges (e.g., along successive stacked faces) whose deletion preserves simplicity, planarity, and 3-connectivity; performing  $S$  such merges yields a graph with the claimed  $(E, F)$ .

## 4.3 External Angle Unit Bounds

From the flatness-based identities in Proposition 4.1, and holding  $V$  fixed, the external angle unit range can be expressed as:

$$M_{\text{ub}} = 10(V - 2), \quad M_{\text{lb}} = \begin{cases} 4V + 6, & V \text{ odd,} \\ 4V + 4, & V \text{ even.} \end{cases}$$

## 4.4 Counting Distinct Combinatorial Configurations

By combining Proposition 4.1 and Corollary 4.2, the total number of distinct  $(F, E)$  configurations attainable by varying  $S$  over its admissible range is:

$$\text{Combinations} = S_{\text{ub}} + 1 = \begin{cases} \frac{3}{2}V - \frac{11}{2}, & V \text{ odd,} \\ \frac{3}{2}V - 5, & V \text{ even.} \end{cases}$$

**Heuristic 4.1** (Realizability across intermediate flatness). *Proposition 4.1 and Lemma 4.1 imply the admissible parity-sensitive ranges for  $E$ ,  $F$ , and  $S$  in Corollary 4.2. What remains heuristic in this work is the claim that every integer  $S$  in the admissible range is realizable by a simple 3-connected planar graph in normal form; see Heuristic Proposition 4.3.*

**Angle units.** One “angle unit” equals the interior angle of a triangle, i.e.,  $180^\circ$ . On a fully triangulated boundary, each triangle contributes exactly one unit and

$$N = F_\Delta = F + S.$$

Under an interior decomposition into  $T$  tetrahedra with  $N_i$  internal gluing triangles, counting triangle units gives

$$N = 4T - 2N_i,$$

since each tetrahedron contributes four triangle units and every internal gluing triangle removes two boundary triangle units by pairing. These two expressions for  $N$  are consistent with Proposition 5.4 and Proposition 4.1: indeed  $F+S = 4T - 2N_i$ . This connection between external angle counts and internal tetrahedral composition will be used in §5 to link internal volumetric parameters directly to external face and edge counts.

## 5 Internal Decomposition and Tetrahedral Estimation

This section shifts from surface validation to internal volumetric structure. We record exact incidence identities governing tetrahedral decompositions of genus-0 polyhedra in normal form, then study how restricted construction rules (SALT+MIE) and surface structure constrain realizability.

**Scope disclaimer.** Throughout, we restrict attention to *normal-form* decompositions: all vertices lie on the boundary, no interior vertices are introduced, and all tetrahedra are glued face-to-face. When we invoke *SALT+MIE*, we mean the further restricted construction class used in §4 (shell-aligned layering; no edge bisections; at most one new interior segment per shell layer).

### 5.1 Determining admissible tetrahedral ranges from polygonal surface data

We consider the following problem: given a closed genus-0 polyhedral surface specified by a multiset of polygonal faces, determine the admissible range of tetrahedral decompositions consistent with purely symbolic (incidence-based) constraints.

#### 5.1.1 Input data and boundary normalization

Let the surface consist of faces with degrees  $\deg f \geq 3$ . From this data we compute:

$$V = \text{number of vertices,} \quad E = \text{number of boundary edges,} \quad F = \text{number of faces.}$$

Define the surface flatness parameter

$$S := \sum_f (\deg f - 3),$$

which equals the number of diagonals in any triangulation of the polygonal faces (without introducing new vertices).

Since triangulating a face of degree  $k$  introduces exactly  $k - 3$  diagonals, summing over faces gives  $S$ . After triangulation, the boundary data become

$$N := F + S \quad (\text{boundary triangles}), \quad E_{\partial} := E + S \quad (\text{boundary edges}).$$

For genus-0 surfaces these satisfy

$$N = 2V - 4, \quad E_{\partial} = 3V - 6,$$

so once  $V$  is fixed the triangulated boundary counts  $(N, E_{\partial})$  are fixed.

### 5.1.2 Interior variables and the SALT+MIE identification

Let

$T$  = number of tetrahedra,  $N_i$  = number of internal gluing triangles,  $S_i$  = number of internal triangulation segments

Here  $S_i$  counts the interior edges needed to fully triangulate the union of internal gluing surfaces. In the SALT+MIE class used in §4, *every interior edge arises as such a triangulation segment*, so  $S_i$  is also the total count of interior edges in the tetrahedral complex. We therefore use  $S_i$  as the interior-edge variable throughout (and do not introduce a separate  $E_i$ ).

### 5.1.3 Exact incidence identities (normal form)

The following identities hold for normal-form tetrahedralizations with triangulated boundary and no interior vertices.

**Triangle incidence.** Each tetrahedron contributes four triangular faces; boundary triangles are used once and internal triangles are shared by two tetrahedra. Hence

$$4T = N + 2N_i. \tag{1}$$

**Euler characteristic.** Let  $E_{\partial}$  denote boundary edges after triangulation, and let  $S_i$  denote interior edges (equivalently: interior triangulation segments in SALT+MIE). The Euler characteristic of the 3-ball gives

$$V - (E_{\partial} + S_i) + (N + N_i) - T = 1. \tag{2}$$

Substituting the genus-0 boundary relations  $N = 2V - 4$  and  $E_{\partial} = 3V - 6$ , (2) simplifies to the exact identity

$$\boxed{T - N_i + S_i = 1.} \tag{3}$$

Appendix B demonstrates that the identity (3) is robust when internal structure arises solely from boundary-induced triangulation (the SALT+MIE setting), and that it fails once interior Steiner points are introduced. Appendix C, by contrast, demonstrates invariance under surface-embedded edge Steiner points.

### 5.1.4 Solution family and feasibility constraints

Equations (1) and (3) parameterize all incidence-admissible triples  $(T, N_i, S_i)$  by the single integer  $T$ . Solving (1) for  $N_i$  and substituting into (3) yields

$$\boxed{N_i(T) = 2T - \frac{N}{2}, \quad S_i(T) = N_i(T) - T + 1 = T - \frac{N}{2} + 1.} \tag{4}$$

Thus, for a fixed polygonal surface (hence fixed  $V$  and fixed  $N = 2V - 4$ ), all admissible tetrahedralizations lie on the one-parameter integer family (4), subject only to nonnegativity:

$$N_i(T) \geq 0, \quad S_i(T) \geq 0.$$

From  $N_i(T) \geq 0$  one obtains the general incidence lower bound

$$T \geq \left\lceil \frac{N}{4} \right\rceil = \left\lceil \frac{2V-4}{4} \right\rceil = \left\lceil \frac{V-2}{2} \right\rceil,$$

which is necessary in any normal-form tetrahedralization. In the restricted SALT+MIE class, the stronger construction minimum  $T_{\min} = V - 3$  is observed (§4), and the ladder family below realizes all intermediate values.

### 5.1.5 Restricted SALT+MIE ranges (construction-based)

Within the SALT+MIE framework of §5 (at most one new interior segment per layer, and the first/last layers cannot host a new segment), one has

$$0 \leq S_i \leq V - 5.$$

Substituting into the ladder relations of §4 gives the construction-based ranges

$$T = V - 3 + S_i, \tag{5}$$

$$N_i = V - 4 + 2S_i, \tag{6}$$

hence

$$T_{\min} = V - 3, \tag{7}$$

$$T_{\max} = 2(V - 4),$$

$$N_{i,\min} = V - 4, \tag{8}$$

$$N_{i,\max} = 3(V - 4) - 2,$$

$$S_{i,\max} = V - 5. \tag{9}$$

These SALT+MIE bounds are not independent: they are linked by the exact identity (3).

## 5.2 Exact interior incidence identities (normal form)

**Proposition 5.1** (Exact 3D Euler link). *Let  $T$  be the number of tetrahedra in a genus-0 tetrahedralization,  $N_i$  the number of internal gluing triangles,  $E_i$  the number of interior edges, and  $V_i$  the number of interior vertices. Then*

$$\boxed{T - N_i + E_i - V_i = 1.}$$

**Proposition 5.2** (Angle units and internal gluings). *Let a genus-0 polyhedron in normal form be tetrahedralized into  $T$  tetrahedra with  $N_i$  internal gluing triangles. After triangulating all boundary faces, the number of boundary triangles is  $N = 2V - 4$ . Counting triangle units gives*

$$4T - 2N_i = N \implies \boxed{N_i = 2T - V + 2.}$$

**Proposition 5.3** (Normal-form specialization). *In normal form,  $V_i \equiv 0$  and every interior edge is an internal triangulation segment; define  $S_i := E_i$ . Then*

$$\boxed{T - N_i + S_i = 1,}$$

and combining with Proposition 5.2 yields

$$\boxed{T = V - 3 + S_i.}$$

These identities are exact and independent of any construction method.

### 5.3 General solution family and incidence bounds

For fixed boundary data (hence fixed  $V$ ), Propositions 5.2–5.3 parameterize all admissible triples  $(T, N_i, S_i)$  by the integer variable  $T$ , subject only to nonnegativity. In particular,

$$N_i(T) = 2T - V + 2, \quad S_i(T) = T - V + 3.$$

From  $N_i \geq 0$  one obtains the general incidence bound

$$T \geq \left\lceil \frac{V-2}{2} \right\rceil,$$

which holds for any normal-form tetrahedralization.

### 5.4 SALT ladder family

Within SALT+MIE, a transparent subfamily is the “ladder” construction where a polygon is decomposed into tetrahedra by the identification of internal triangular gluing faces one by one. For  $k = 0, \dots, V-5$ ,

$$T_k = V - 3 + k, \quad N_{i,k} = V - 4 + 2k, \quad S_{i,k} = k,$$

and  $T_k - N_{i,k} + S_{i,k} = 1$  holds exactly.

For fixed  $V$ , the ladder construction realizes exactly  $V-4$  distinct admissible triples  $(T, N_i, S_i)$  under SALT+MIE.

**Heuristic 5.1** (Internal ranges and configuration ladder). *The ranges for  $(T_{\min}, T_{\max})$ ,  $(N_{i,\min}, N_{i,\max})$ , and  $S_{i,\max}$ , together with the ladder*

$$T_k = V - 3 + k, \quad N_{i,k} = V - 4 + 2k, \quad S_{i,k} = k \quad (0 \leq k \leq V - 5),$$

*match all worked examples and constructions tested to date, but are presently justified empirically rather than by a complete classification.*

### 5.5 Empirical truncation at fixed $V$

Although the ladder exhausts the algebraic SALT+MIE range, realizability at fixed  $V$  depends on the external surface structure  $(E, F, S)$ . Table 2 (for  $V = 8$ ) exhibits a sharp compression: as surface flatness  $S$  increases, progressively fewer ladder rungs are realized. For example, when  $S = 6$  (the cube), only  $T = 5$  and  $T = 6$  occur, despite the algebraic allowance of  $T = 7, 8$ . Thus the effective maximum is strictly below the incidence ceiling.

Table 2: Valid  $(T, N_i, S_i)$  configurations observed at  $V = 8$  under SALT+MIE, grouped by external flatness  $S$ . Here  $E$  denotes the number of boundary edges prior to triangulating non-triangular faces. For fixed  $V = 8$ , the triangulated boundary satisfies  $E + S = 3V - 6 = 18$ .

$E$	$S$	$T$	$N_i$	$S_i$
18	0	5	4	0
18	0	6	6	1
18	0	7	8	2
18	0	8	10	3
17	1	5	4	0
17	1	6	6	1
17	1	7	8	2
16	2	5	4	0
16	2	6	6	1
15	3	5	4	0
15	3	6	6	1
14	4	5	4	0
14	4	6	6	1
13	5	5	4	0
13	5	6	6	1
12	6	5	4	0
12	6	6	6	1

From these configurations, the following empirical tendencies are observed for eight-vertex polyhedra:

- When  $S = 0$ : all  $V - 4$  ladder configurations are realized.
- When  $S = 1$ : the top ladder rung ( $S_i = S_{i,\max}$ ) is not realized.
- When  $2 \leq S \leq S_{i,\max}$ : only the two lowest ladder rungs ( $S_i = 0, 1$ ) are realized.

This compression is empirical and specific to  $V$ ; it reflects the interaction between boundary structure and volumetric packing rather than a failure of the incidence identities.

## 5.6 Flexibility and Inflexibility of Internal Arrangements at Fixed $V$

The preceding sections establish admissible ranges for the number of tetrahedra  $T$  and internal gluing triangles  $N_i$  for a polyhedron with fixed boundary vertex count  $V$  under the SALT+MIE construction rules. However, these bounds alone do not distinguish between configurations that admit multiple internal realizations and those that are structurally rigid. In this section, we introduce a qualitative distinction between *inflexible* and *flexible* internal arrangements, based on whether the surface triangulation budget  $S$  can vary while  $V$  and  $T$  are held fixed.

### 5.6.1 Definition: $S$ -flexibility

Fix a boundary vertex count  $V$  and a tetrahedral count  $T$ . We say that a configuration is  *$S$ -inflexible* if all valid SALT+MIE realizations with these fixed values of  $(V, T)$  admit the same value of  $S$ . Conversely, a configuration is  *$S$ -flexible* if there exist two valid realizations with the same  $(V, T)$  but different values of  $S$ .

Intuitively,  $S$ -inflexibility corresponds to a boundary and interior structure that forces a unique surface triangulation compatible with a valid tetrahedral fill, while  $S$ -flexibility indicates the presence of discrete triangulation choices that do not alter the global counts  $V$  or  $T$ .

### 5.6.2 Inflexible class: bipyramidal configurations

The canonical examples of  $S$ -inflexible arrangements are *bipyramidal configurations*. These consist of two apex vertices (one “above” and one “below”) connected to all vertices of a central polygonal cycle. All faces are triangular, and the interior tetrahedra fan out from the central polygon in a forced manner.

For such configurations:

- the induced tetrahedral adjacency structure is fixed,
- no local rearrangement of internal gluing surfaces is possible without changing either  $V$  or  $T$ ,
- the surface triangulation budget  $S$  is uniquely determined (typically  $S = 0$ ).

An explicit example is the case  $(V, T) = (8, 8)$ , where the only realizable configuration is a hexagonal bipyramid. In this case, no alternative triangulation of the surface exists that is compatible with a valid tetrahedral decomposition, and the configuration is strictly  $S$ -inflexible.

### 5.6.3 First deviation: single-vertex departure from bipyramidity

Flexibility first appears when the bipyramidal structure is minimally perturbed. Specifically, if one vertex leaves the equatorial polygon and is reassigned to either the upper or lower apex side, the central polygon is reduced by one vertex. One side of the polyhedron remains a pyramid, while the opposite side now contains a single quadrilateral face.

This quadrilateral face admits exactly two triangulations, yielding two distinct but valid surface configurations:

- one realization with  $S = 0$ ,
- one realization with  $S = 1$ .

Crucially, both realizations share the same values of  $(V, T)$ . Thus, this class represents a *minimally flexible* arrangement, with exactly one discrete degree of freedom in  $S$ . The interior accommodates one fewer tetrahedron than the corresponding pure bipyramid, but remains otherwise tightly constrained.

### 5.6.4 Higher deviations: increasing flexibility

Additional flexibility arises when further vertices leave the equatorial polygon. For example:

- two vertices may be reassigned to the same side, producing a pentagonal face;
- or one vertex may move upward while another moves downward, producing a quadrilateral face on each side.

Each non-triangular face introduces an independent triangulation choice. As a result, the set of admissible values of  $S$  grows, while  $V$  and  $T$  remain fixed. These configurations are genuinely  $S$ -flexible, exhibiting multiple realizable internal arrangements and a nontrivial range of surface triangulation budgets.

## 5.7 Interpretation

This progression suggests a natural stratification of configurations at fixed  $V$ :

$$\text{bipyramidal (rigid)} \rightarrow \text{single-defect (minimally flexible)} \rightarrow \text{multi-defect (flexible)}.$$

In this view, bipyramidal configurations form the rigid core of the admissible space, while flexibility emerges precisely as vertices are removed from the equatorial cycle. Each such departure introduces a higher-degree face and hence an additional discrete triangulation choice, reflected in the admissible range of surface flatness  $S$ .

This distinction clarifies why the admissible SALT+MIE bounds alone do not determine  $T$  or  $S$  uniquely: realizability within those bounds depends sensitively on the internal combinatorial structure, not solely on boundary counts.

**Remark (Incidence-Gated Transitions, Bipyramidal Rigidity, and Boundary Flexibility).** Although the analysis throughout this work is entirely symbolic, it is often helpful to imagine vertices as concrete points in space and tetrahedra as occupying volume. This geometric picture is not essential, but it helps explain why certain discrete effects appear abruptly rather than gradually.

A key point is that the equatorial “belt” in a bipyramidal configuration need not be coplanar. Coplanarity is a red herring: what actually governs admissibility is the pattern of *external boundary edges* and *internal gluing segments*. As long as these incidence relations are preserved, the belt vertices can ripple or kink freely in space without any effect on the tetrahedral count or on other boundary quantities (edges and faces). Geometry supplies continuous freedom within each combinatorial state.

From this perspective, bipyramidal configurations occupy a special extremal position. Their rigidity is geometrically obvious: two apices constrain a belt of vertices so tightly that there is essentially no slack. However, this rigidity is largely invisible at the level of surface incidence counts alone. In informal terms, bipyramids are often mistaken for “flexible” objects combinatorially, even though they are maximally constrained volumetrically. This is why, if one insists on geometric metaphors for rigidity, the usual description of inflexible objects as “squares” is misleading: squares are flexible in triangulated settings and signal at least a degree of boundary flexibility, whereas bipyramids are not.

Departures from bipyramidity occur through discrete reclassifications of vertex roles rather than smooth geometric limits. The primitive defect is not an apex becoming coplanar with the belt, but the reassignment of a *belt vertex*. When a single belt vertex ceases to attach symmetrically to both apices, remaining connected to only one apex while acquiring additional lateral connections, the belt shortens by one, an internal gluing segment is lost, and exactly one tetrahedron disappears. This produces the first unit of variability: two triangular faces may unite to form a boundary quadrilateral ( $S = 1$ ), the tetrahedral count drops by one, and the boundary geometry remains otherwise flexible, but now within a new combinatorial state.

A stronger transition occurs if deformation proceeds far enough that an *apex-apex edge* appears. In this regime the belt is no longer merely reclassified locally; it is shortened more substantially, and multiple tetrahedra are lost simultaneously. In an eight-vertex system, for example, this transition produces a loss of two or three tetrahedra (depending on how the polygon is decomposed) relative to the bipyramidal maximum. These changes are discrete and unavoidable: intermediate geometric states do not register combinatorially because the system skips them by reorganizing its incidence structure.

This behavior illustrates a general asymmetry between boundary and interior. Continuous geometric variation of the boundary can induce discrete changes in interior capacity, while fixing the combinatorial structure of the tetrahedral decomposition leaves substantial freedom in the realization of the boundary. The resulting “quantized” behavior of tetrahedral and boundary counts is not a physical effect, but a consequence of incidence-gated admissibility: counts remain constant under arbitrary rippling until a gate is crossed, at which point they jump.

## 5.8 Inferring external structure from internal decomposition

This subsection relates the internal tetrahedral decomposition of a genus-0 polyhedron to the combinatorics of its boundary surface. We recall the exact topological identities for tetrahedralizations of a 3-ball and their normal-form specialization (already established in Propositions 5.1–5.3), then record a useful incidence-based rule-of-thumb for reconstructing  $(V, E, F)$  from interior decomposition data.

### 5.8.1 Exact Euler link and normal-form specialization

For any tetrahedral complex filling a 3-ball, the exact identity (Proposition 5.1)

$$T - N_i + E_i - V_i = 1$$

always holds. In the normal form adopted throughout this manuscript,  $V_i \equiv 0$  and every interior edge is an internal triangulation segment, so  $E_i = S_i$  and hence (Proposition 5.3)

$$\boxed{T - N_i + S_i = 1}.$$

Moreover, after triangulating all boundary faces, triangle incidence gives (Proposition 5.2)

$$\boxed{N_i = 2T - V + 2}.$$

Together these identities link the interior parameters  $(T, N_i, S_i)$  to the boundary vertex count  $V$  in a purely symbolic way.

### 5.8.2 Heuristic incidence formulas for external structure

The next statement is *not* a general topological law; it is an incidence calculation that assumes:

1. no interior Steiner vertices ( $V_i = 0$ ),
2. all internal adjacencies occur along triangular faces,
3.  $S = \sum_f (\deg f - 3)$  is the face-degree excess (equivalently the number of boundary triangulation diagonals),
4.  $S_i$  counts internal triangulation segments completing gluing surfaces.

**Heuristic Proposition 5.4** (Boundary counts from interior decomposition). *Assume a genus-0 decomposition into  $T$  tetrahedra without interior Steiner vertices, where internal adjacencies occur only along triangular faces; let  $N_i$  be the number of internal gluing triangles,  $S$  the number of coplanarity merges on the boundary, and let  $S_i$  denote the number of interior edges. Then the boundary satisfies*

$$E = 6T - 3N_i - S, \quad F = 4T - 2N_i - S, \quad V = 4T - 3N_i + 2S_i.$$

*Justification.* For a fully triangulated boundary,  $F_\Delta = 4T - 2N_i$  and  $E_\Delta = \frac{3}{2}F_\Delta = 6T - 3N_i$  by triangle incidence. Coplanarity merges reduce both  $E_\Delta$  and  $F_\Delta$  by  $S$ , yielding the displayed formulas for  $E$  and  $F$ . The  $V$ -formula is algebraically equivalent to the exact identities  $N_i = 2T - V + 2$  and  $T - N_i + S_i = 1$  (Propositions 5.2–5.3), hence consistent.

**Sanity check.** In normal form,  $T - N_i + S_i = 1$  (Proposition 5.3), so the above formulas automatically satisfy  $V - E + F = 2$  after substitution.

### 5.8.3 Heuristic extension of Euler’s characteristic

Substituting the heuristic expressions of Proposition 5.4 into  $V - E + F$  gives

$$V - E + F = 2(T - N_i + S_i).$$

**Heuristic 5.2** (Extended Euler-type identity). *Under the hypotheses of Proposition 5.4,*

$$V - E + F = 2(T - N_i + S_i).$$

*Note: This is an incidence packaging of the boundary formulas above; it is not asserted as a general topological law. In normal form,  $T - N_i + S_i = 1$  (Proposition 5.3), hence  $V - E + F = 2$  as expected.*

Appendix F compiles all identities and bounds derived in Sections 4 and 5.

## 6 A Combinatorial Method for Testing 3D Polygonal Enclosure and Polyhedral Feasibility

Section 6 formalizes a combinatorial method to assess polygon lists for enclosure feasibility, including a “flatness threshold” test. The method operates on a list of polygon types and their frequencies (e.g., 12 pentagons, 20 hexagons), without requiring coordinates or spatial modeling. It proceeds in several steps:

**Step 1: Polygon Frequency:** Define the count of each polygon type  $P_k$ .

**Step 2: Total Internal Angle Units (N):** Each  $k$ -gon contributes  $(k - 2)$  angle units of  $180^\circ$ . Compute total:

$$N = \sum_{k=3}^n (k - 2) P_k$$

**Step 3: Vertex Count Estimate (V)** For any genus-0 polyhedron in normal form (simple 3-connected boundary; no edge bisections or interior boundary vertices), the vertex count is governed by a direct formula in terms of the face-degree counts.

**Proposition 6.1.** *Let  $P_k$  denote the number of faces of degree  $k$ , and define*

$$N = \sum_{k \geq 3} (k - 2) P_k.$$

*Then for any finite simple graph with a 2-cell embedding in  $S^2$  (genus 0),*

$$V = \frac{N}{2} + 2$$

*Proof.* From the face-edge incidence relation,

$$2E = \sum_{k \geq 3} k P_k = \sum_{k \geq 3} (k - 2) P_k + 2 \sum_{k \geq 3} P_k = N + 2F.$$

By Euler's formula  $V - E + F = 2$ , substituting  $E = (N + 2F)/2$  gives

$$V - \frac{N + 2F}{2} + F = 2 \quad \Rightarrow \quad V - \frac{N}{2} = 2,$$

and hence  $V = \frac{N}{2} + 2$ .

**Corollary 6.1** (Integer feasibility check). *If  $N$  is odd, then  $V$  is non-integer and no valid genus-0 polyhedron in normal form with such a face-degree distribution can exist.*

*Remark (origin of the formula).* An earlier derivation produced the more elaborate rational form

$$V = \frac{2M_{\text{total}} - N(2S_{\text{total}} + 10)}{M_{\text{total}} - 5N},$$

with

$$M = \sum_{k \geq 3} (k + 2) P_k, \quad S = \sum_{k \geq 3} (k - 3) P_k,$$

arising from edge-face incidence counts and the extremal relation  $E = 3V - 6 - S$ . Under the genus-0, normal-form constraints, one has  $M - 5N = -4S$ , which causes the above expression to collapse identically to  $V = \frac{N}{2} + 2$  for all values of  $S$ . This shows that the vertex count is *independent* of flatness in this setting.

*Historical derivation*

Let  $P_k$  be the number of  $k$ -gonal faces, and define

$$N = \sum_{k \geq 3} (k - 2) P_k, \quad M = \sum_{k \geq 3} (k + 2) P_k, \quad S = \sum_{k \geq 3} (k - 3) P_k, \quad F = \sum_{k \geq 3} P_k.$$

From

$$2E = \sum_{k \geq 3} k P_k, \quad 2E = 3F + S,$$

we find

$$M = (2E) + 2F, \quad N = (2E) - 2F,$$

and hence

$$E = \frac{M + N}{4}, \quad F = \frac{M - N}{4}, \quad M - 5N = -4(2E - 3F) = -4S.$$

With  $E = 3V - 6 - S$  (Proposition 4.1), we have

$$\frac{M + N}{4} = 3V - 6 - S \implies V = \frac{M + N + 24 + 4S}{12}.$$

Substituting  $M = 5N - 4S$  yields

$$V = \frac{N}{2} + 2.$$

Thus the simple form follows unconditionally from the general counts.

**Step 4: Face-degree excess (flatness)  $S$ :**

$$S := \sum_{k \geq 3} (k - 3) P_k.$$

**Step 5: Total Face Count (F):**

$$F = \sum_{k=3}^n P_k$$

**Step 6: Edge count (E):**

$$E = 3V - 6 - S.$$

Equivalently, after triangulation one has  $F_{\Delta} = F + S$  and  $E_{\partial} = E + S$ , and the triangulated incidence identity

$$2E_{\partial} = 3F_{\Delta} \quad \text{i.e.} \quad 2(E + S) = 3(F + S)$$

holds.

**Step 7: Euler's Formula Check:**

$$V - E + F = 2$$

If  $V - E + F$  does not equal to 2, then the set of polygon types does not enclose a valid 3D volume.

**Step 8: Flatness Constraint:**

$$S_{\text{lb}} = 0$$

$$S_{\text{ub}} = \begin{cases} \frac{3}{2}V - \frac{13}{2} & \text{if } V \text{ is odd} \\ \frac{3}{2}V - 6 & \text{if } V \text{ is even} \end{cases}$$

$$S_{\text{diff}} = S_{\text{ub}} - S$$

If  $S > S_{\text{ub}}(V)$ , the face-degree excess exceeds the parity/degree upper bound implied by  $\delta(G) \geq 3$ , so no such genus-zero polyhedral graph can exist. Loosely, one may say the proposed surface is “*too flat (combinatorially) to enclose*”.

**Summary of Practical Application (Appendix D)** The combinatorial method introduced in this paper has been applied to a range of polygonal configurations, demonstrating its capacity to correctly validate known polyhedra, reject over-flattened ones, and expose structurally deceptive false positives. These worked examples include the cube, the square pyramid, and the regular dodecahedron, each of which passes all symbolic checks and matches known geometry. For example, the decomposition of the cube yields five tetrahedra which aligns with a known meshing scheme producing four right tetrahedra at its corners and a central regular tetrahedron [7]. In contrast, a configuration of 36 hexagons fails the flatness threshold, while a less intuitive case, two hexagons and four triangles, passes all algebraic constraints but appears unrealizable in  $\mathbb{R}^3$ , highlighting the symbolic method’s limits. Intriguingly, substituting two triangles with one square in that borderline case causes the structure to fail the flatness test entirely, revealing a sharp combinatorial threshold. Such substitutions may serve as diagnostic probes for detecting “brittleness” in enclosure feasibility. These examples reinforce the method’s utility as both a filtering tool for polyhedral candidates and a lens through which to explore the fine boundary between combinatorial sufficiency and geometric necessity.

## 7 Symmetry Between Face- and Vertex-Type Combinatorics

This section investigates the symmetry between face types and vertex valencies, drawing attention to a duality often noted but rarely operationalized in enclosure logic. In analyzing polyhedra from a combinatorial standpoint, we observe a notable parallelism between the types of faces and the types of vertices.

### 7.1 Face Types and Vertex Types

Each face of a polyhedron is defined by the number of its edges (or equivalently, the number of vertices around it), while each vertex is defined by the number of edges meeting at that point. These quantities are known as:

- **Face degrees:** the number of edges surrounding a face,
- **Vertex valencies:** the number of edges incident to a vertex.

For a polyhedron with  $V$  vertices,  $E$  edges, and  $F$  faces, we always have the exact incidence identity

$$\sum_{i=1}^F d_i = 2E = \sum_{j=1}^V v_j,$$

where  $d_i$  is the degree of the  $i$ -th face and  $v_j$  is the valency of the  $j$ -th vertex. This face–vertex symmetry is emphasized in Grünbaum’s treatment of polyhedral duality [6], where vertex valencies and face degrees are shown to reflect a deeper structural reciprocity across convex forms. It reflects a basic balance: each edge is shared by two faces and connects two vertices, hence contributes twice to the totals.

### 7.2 Observed Symmetry and Interpretation

From empirical examination and combinatorial modeling, I notice that:

- The range of face types (triangle, quadrilateral, pentagon, etc.) mirrors the range of vertex types (valency 3, 4, 5, etc.).
- The minimum possible face or vertex type is generally 3 (a triangle or trivalent vertex), which is necessary for a polyhedron to be enclosed.
- The maximum number of edges in a face or incident edges at a vertex is bounded by the number of vertices, typically less than  $V$ .

This observation does not suggest a strict one-to-one mapping but highlights a structural analogy:

- When enumerating or constructing valid polyhedra, both sets of types must satisfy the same total:

$$\text{Total face degrees} = \text{Total vertex valencies} = 2E.$$

- This constrains generation algorithms and supports validation strategies.
- It provides a balanced perspective when analyzing polyhedra from the inside (vertices) or outside (faces).

Though rooted in standard topological rules, this symmetry has not been prominently emphasized in the literature as a guiding structure. It suggests an intuitive, combinatorial harmony between internal and external complexity.

### 7.3 Face-Type Combinatorial Constraints

We now narrow down the valid face-type combinations in a polyhedron vertex count  $V$ , edge count  $E$ , face count  $F$ , and external flatness  $S$ .

**Face-Type Limit Rule.** In a polyhedral graph with  $V$  vertices, any face can have at most  $V - 1$  edges, since its boundary is a simple cycle and therefore cannot visit all  $V$  vertices without repetition.

**Equations for Face-Type Combinations.** For given values of  $F$ ,  $E$ , and  $S$ , the face-type variables must satisfy:

$$\begin{aligned} F_3 + F_4 + F_5 + \dots &= F && \text{(total number of faces),} \\ 3F_3 + 4F_4 + 5F_5 + \dots &= 2E && \text{(edge-face incidence),} \\ (3-3)F_3 + (4-3)F_4 + (5-3)F_5 + \dots &= S && \text{(external triangulation segments).} \end{aligned}$$

All solutions must be non-negative integers.

**Worked Example** ( $V = 6$ ,  $S = 2$ ,  $E = 10$ ,  $F = 6$ ). Allowed face types: triangles, quadrilaterals, and pentagons (up to 5 sides). Valid integer solutions:

- $F_3 = 4$ ,  $F_4 = 2$ ,  $F_5 = 0$  (4 triangles, 2 quadrilaterals),
- $F_3 = 5$ ,  $F_4 = 0$ ,  $F_5 = 1$  (5 triangles, 1 pentagon).

Both satisfy:

$$\begin{aligned} F_3 + F_4 + F_5 &= 6 \\ 3F_3 + 4F_4 + 5F_5 &= 20 \\ F_4 + 2F_5 &= 2. \end{aligned}$$

### 7.4 Vertex-Type Combinatorial Constraints

We now narrow down the valid vertex-type combinations in a polyhedron with total vertex count  $V$  and edge count  $E$ .

**Vertex Type System of Equations.** Every valid vertex-type configuration must satisfy:

$$\begin{aligned} V_3 + V_4 + V_5 + \dots &= V && \text{(vertex count)} \\ 3V_3 + 4V_4 + 5V_5 + \dots &= 2E && \text{(edge incidence)} \\ V_3 + 2V_4 + 3V_5 + \dots &= 2E - 2V && \text{(since } \sum_j (\deg v_j - 2) = 2E - 2V). \end{aligned}$$

All variables must be non-negative integers, and the maximum degree allowed is  $V - 1$ .

**Worked Example** ( $V = 6, E = 10, S = 2, T = 3$ ). Solutions include:

- $V_3 = 4, V_4 = 2, V_5 = 0,$
- $V_3 = 5, V_4 = 0, V_5 = 1.$

Both satisfy all constraints.

**Worked Example: A Likely Non-Realizable Configuration.** Given  $V = 6, E = 11, S = 1, T = 3,$  valid solutions include:

Config	$V_3$	$V_4$	$V_5$
1	2	4	0
2	3	2	1
3	4	0	2

Configs 1 and 2 appear realizable; Config 3 fails embedding. The corresponding face-type configuration is  $a = 6$  (triangles),  $b = 1$  (quadrilateral), which matches edge counts but resists geometric embedding.

## 7.5 Limitations and Realizability Filters

This illustrates a key limitation: satisfying combinatorial constraints does not guarantee embeddability in three-dimensional space. As Grünbaum notes, only graphs that are planar and 3-connected can be realized as convex 3D polyhedra, a result due to Steinitz [6].

To reduce false positives, one may introduce heuristic filters:

- Bounding the number of high-valency vertices relative to the number of tetrahedra,
- Angle feasibility checks,
- Limits on repeated vertex incidence across tetrahedra.

Such filters are not definitive, but they help identify configurations that are combinatorially possible yet geometrically implausible.

## 7.6 Summary

In summary, the structural symmetry between face-type and vertex-type combinatorics provides a unifying framework. The parallel systems of equations show that both perspectives encode the same edge-incidence information while imposing complementary feasibility conditions. This dual viewpoint clarifies why some integer solutions admit realizable polyhedra while others fail, highlighting the balance between external and internal complexity in polyhedral structures.

# 8 On All Likely Configurations of a Polyhedron and The Limits of Combinatorial Realizability

Section 8 explores a possible route for exploring all likely configurations of a polyhedron defined by a number of vertices and derived surface flatness by utilizing an unrestricted partition function  $p(S)$ . As shown in earlier sections, every valid polyhedron of  $V$  vertices is characterized by two distinct combinatorial structures:

- The external structure:  $(F, E, M, S)$ . For a polyhedron of vertices  $V$ , these complements have a total number of combinations =  $\begin{cases} \frac{3}{2}V - \frac{11}{2} & \text{if } V \text{ is odd} \\ \frac{3}{2}V - 5 & \text{if } V \text{ is even} \end{cases}$
- The internal structure:  $(T, N_i, S_i)$ . For a polyhedron of vertices  $V$ , these complements have a total number of combinations of  $V - 4$

I now define a function that estimates a lower bound on the number of valid combinations between these two sets for a given vertex count  $V$ . We denote this conservative estimate by  $\text{Combinations}_{\text{S}_{\min}}(V)$ . This count reflects how many internally and externally compatible sets of structures exist, without specifying the actual types of those structures (face-types and vertex-types). Refining this lower bound by characterizing the persistence of internal multiplicity as a function of  $S$  remains an open combinatorial problem.

### 8.1 Conservative Estimate for Structure Pair Combinations

$$\text{Combinations}_{\text{S}_{\text{lb}}}(V) = \begin{cases} \frac{1}{2}V^2 - 3V + 5, & \text{if } V \text{ is even,} \\ \frac{1}{2}V^2 - 3V + \frac{9}{2}, & \text{if } V \text{ is odd.} \end{cases}$$

**Derivation.** Fix a vertex count  $V \geq 4$ . The external flatness parameter  $S$  ranges over

$$S = 0, 1, \dots, S_{\text{ub}}(V), \quad S_{\text{ub}}(V) = 3V - 6 - \left\lceil \frac{3V}{2} \right\rceil = \begin{cases} \frac{3V}{2} - 6, & V \text{ even,} \\ \frac{3V}{2} - \frac{13}{2}, & V \text{ odd.} \end{cases}$$

For each fixed  $S$ , the internal tetrahedral count is constrained by the internal ladder bounds

$$T_{\min}(V) = V - 3 \quad \text{and} \quad T_{\max}(V, S) = 2V - 8 - S.$$

Thus, at the level of global internal invariants, the number of admissible integer values of  $T$  compatible with a given  $S$  is at most

$$T_{\max}(V, S) - T_{\min}(V) + 1 = (2V - 8 - S) - (V - 3) + 1 = V - 4 - S.$$

In particular, as  $S$  increases, the admissible  $T$ -range shrinks linearly. At  $S = 0$  (fully triangulated boundary), there exist polyhedra that realize the full ladder of internal invariant values  $(T, N_i, S_i)$ , with the bipyramid-prism family attaining the maximal value  $T_{\max}$ .

To obtain a conservative macro-level pairing count, we require only that at least one internally compatible invariant triple exists for each admissible value of  $S$ , even after the  $T$ -interval collapses. Writing this as a capped count gives

$$N_{\text{int}}(V | S) = \max\{V - 4 - S, 1\} = \max\{2V - 8 - S - (V - 3) + 1, 1\}.$$

Therefore the total number of compatible external-internal macro-pairs is

$$\sum_{S=0}^{S_{\text{ub}}} N_{\text{int}}(V | S) = \sum_{S=0}^{V-5} (V - 4 - S) + \sum_{S=V-4}^{S_{\text{ub}}} 1.$$

The first term is a triangular sum,

$$\sum_{S=0}^{V-5} (V - 4 - S) = (V - 4) + (V - 5) + \dots + 1 = \frac{(V - 4)(V - 3)}{2},$$

and the second term contributes a linear tail of length  $S_{\text{ub}} - (V - 4) + 1$ . Substituting the parity form of  $S_{\text{ub}}$  and simplifying yields

$$\text{Combinations}_{\text{S}_{\text{lb}}}(V) = \begin{cases} \frac{1}{2}V^2 - 3V + 5, & V \text{ even,} \\ \frac{1}{2}V^2 - 3V + \frac{9}{2}, & V \text{ odd.} \end{cases}$$

Here the quadratic leading term arises from summing the linearly shrinking internal ladder across  $S$ , while any multiplicity of realizations for a given  $(V, S, T)$  affects only lower-order corrections beyond this macro-invariant count.

It is worth emphasizing again that this estimate is intentionally conservative. As illustrated in Table 2 for  $V = 8$ , multiple distinct internal configurations may persist even after the nominal  $T$ -interval has ceased to shrink linearly with  $S$ . Such persistence increases the true number of compatible structure pairs beyond the value predicted by  $\text{Combinations}(V)$  and indicates that the present formula provides a lower bound rather than an exact count.

**Remark (tail persistence and decomposition pathways).** Table 2 shows that the “tail” regime in  $S$  need not collapse to a single internal invariant triple. For example, at  $V = 8$  the cube admits a  $T = 5$  decomposition obtainable by successive “shaving” moves, but also admits  $T = 6$  decompositions obtained by first partitioning the volume into two hexahedral blocks and then tetrahedralizing each block (three tetrahedra per block). Both outcomes satisfy the same global SALT+MIE constraints, but they differ in  $(T, N_i, S_i)$ , indicating that the multiplicity of internal states at large  $S$  is a genuine structural feature rather than noise. Whether this tail multiplicity grows with  $V$  (thickening tails) or collapses as  $S \rightarrow S_{\text{ub}}(V)$  is left to future enumeration and experimentation.

Numerical values of  $\text{Combinations}_{\text{lb}}(V)$  for  $4 \leq V \leq 20$ , together with a graphical illustration of its quadratic growth, are given in Appendix E. Notably, this lower-bound count grows only polynomially in  $V$ , whereas the number of admissible face-type configurations grows combinatorially, as it is controlled by the cumulative sum of integer partition counts  $\sum_{S=0}^{S_{\text{ub}}} p(S)$ , as elaborated in the following section.

When attempting to uncover the actual face-type and vertex-type configurations corresponding to a specific polyhedron defined by vertex count  $V$ , triangulation segment count  $S$ , and tetrahedron count  $T$ , the procedures described in Section 7 should be applied. These methods allow one to solve for specific polygonal face arrangements and converge to vertex degree structures that are compatible with a given global combinatorial configuration.

It is important to emphasize that satisfying all combinatorial constraints does not necessarily guarantee spatial realizability of all proposed configurations. This limitation is most apparent in the vertex-type integer combinations but may extend to other aspects of the framework as well. Some solutions that are valid in integer space may still be non-embeddable in three-dimensional geometry due to overlap or topological obstruction. Realizability remains a geometric problem. One that combinatorics alone cannot always resolve.

## 8.2 Estimating the Upper Bound from Flatness and Face Combinations

While previous sections emphasize compatibility between internal and external combinatorics, it is also useful to estimate an upper bound of possible polyhedral configurations based solely on the total surface angle budget. In contrast to a full combinatorial analysis of vertex and edge constraints, this method estimates the number of ways one can arrange polygonal faces on a polyhedral surface using only the flatness range of the surface. It does not take into account local realizability constraints, such as vertex incidence or internal fillability by tetrahedra. As it doesn’t account for vertex types, it serves as a partial initial upper-bound estimate of surface complexity.

## 8.3 Method Outline

### Step 1: Compute the flatness range

Define the triangulation segment budget  $S$ , where  $S = 0$  corresponds to a surface composed entirely of triangles (i.e., zero extra flatness beyond minimal curvature), and larger values of  $S$  correspond to the inclusion of increasingly flat faces (e.g., quadrilaterals, pentagons). The minimum is always  $S_{\text{lb}} = 0$ , corresponding to the fully triangulated case. The maximum possible number of triangulation-equivalent segments  $S_{\text{ub}}$  depends on the number of vertices  $V$  and follows the previously mentioned parity-sharp linear functions:

$$S_{\text{ub}} = \begin{cases} \frac{3}{2}V - \frac{13}{2} & \text{if } V \text{ is odd} \\ \frac{3}{2}V - 6 & \text{if } V \text{ is even} \end{cases}$$

### Step 2: Enumerate face-type combinations using integer partitions

Each valid configuration of polygonal face types can be expressed as an integer partition of  $S$ , where each polygon type contributes a fixed number of “excess segments” relative to a triangle:

- A quadrilateral contributes 1,
- A pentagon contributes 2,
- And so on.

Thus, every value of  $S \in [0, S_{\text{ub}}]$  corresponds to a number of integer partitions under these constraints. The total number of valid polygonal configurations at a given  $V$  is then equal to the sum of these partition counts from  $S_{\text{lb}}$  to  $S_{\text{ub}}$ . If no restriction is placed on the number of polygon sides, then this count becomes equivalent to the unrestricted partition function  $p(S)$ , a classical object in number theory that enumerates the number of ways to write  $S$  as a sum of positive integers (ignoring order) [2]. The partition function begins:

$$p(S) = \{1, 1, 2, 3, 5, 7, 11, 15, 22, 30, 42, \dots\}$$

Therefore, for a given vertex count  $V$ , the number of distinct face-type combinations is:

$$\sum_{S=0}^{S_{\text{ub}}} p(S)$$

For instance, for  $V = 5$ , I compute  $S_{\text{ub}} = 1$ , and the number of valid configurations is:

$$p(0) + p(1) = 1 + 1 = 2$$

**Step 3: Compute total number of face-type combinations** Sum all partition counts (unrestricted) across the flatness range. The resulting total gives an upper bound on the number of distinguishable surface configurations for a polyhedron with  $V$  vertices, assuming only the flatness constraint.

Table 3: Lower and upper bounds on total external flatness  $S$  and the resulting upper bound on admissible face-type combinations, as a function of vertex count  $V$ , under the symbolic enclosure constraints.

$V$	$S_{\text{lb}}$	$S_{\text{ub}}$	Face-type combinations (upper bound)
4	0	0	1
5	0	1	2
6	0	3	7
7	0	4	12
8	0	6	30
9	0	7	45
10	0	9	97
11	0	10	139
12	0	12	272
13	0	13	373
14	0	15	684
15	0	16	915
16	0	18	1597
17	0	19	2087
18	0	21	3506
19	0	22	4508
20	0	24	7338

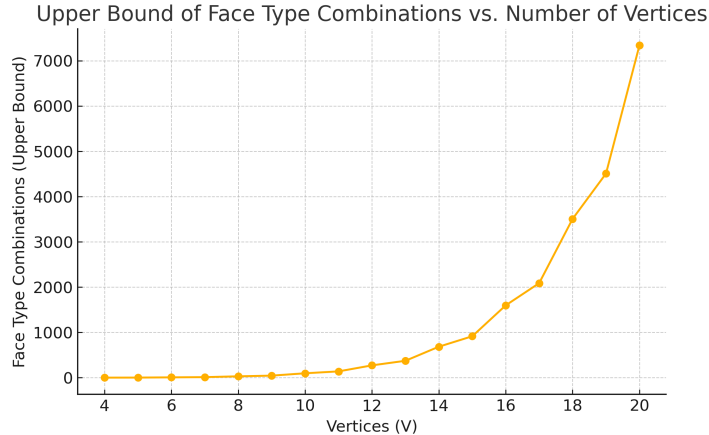


Figure 4: Upper bound of face type combinations as a function of vertex count.

This curve provides an upper bound on the number of surface configurations derivable from face configurations for each vertex count  $V$ , assuming only the flatness constraint is satisfied. It does not account for limitations imposed by vertex-type configurations, or tetrahedral fillability. This is demonstrated in *Appendix A*, as different vertex-type configurations can exist for the same face configuration. Nonetheless, it offers a fast and interpretable way to explore surface complexity based solely on flatness and consequent face composition.

After determining the number of necessary triangles to achieve closure at a desired vertex count, each potential face-type configuration generated via this enumeration can then be filtered or corrected by the stricter combinatorial criteria, such as the one outlined in Section 6 (“A Combinatorial Method for Testing 3D Polygonal Enclosure and Polyhedral Feasibility”). Accordingly, adjustments, such as the addition or removal of triangular faces, can be made to align each configuration with more realizable polyhedral enclosures.

**Step 4: Refine with restricted partitions** If a maximum polygon side count  $k_{\max}$  is imposed (such as limiting the use of hexagons or excluding higher-order polygons) the enumeration becomes a case of *restricted integer partitions*, where only parts of size  $\leq k_{\max} - 3$  are allowed. This constraint reflects that each non-triangular face contributes a specific number of excess triangulation segments. Restricted partitions offer a more realistic estimate by excluding configurations that rely on geometrically unlikely face types. For example, limiting the count of hexagons in some configurations prevents overcounting face combinations that cannot physically tile a polyhedral surface. By summing the number of valid restricted partitions for each value of  $S = 0$  to  $S_{\text{ub}}$ , I obtain a tighter upper bound on the number of feasible face-type combinations, filtering out many false positives that are combinatorially valid but geometrically unconstructible.

## 9 Discussion: Internal Validity, External Limits, and Future Directions

This study has introduced a symbolic, coordinate-free framework for assessing the enclosability and internal structure of 3D polyhedra. By relying solely on integer arithmetic, triangle counts, and combinatorial rules, the method offers a new approach to reasoning about polyhedral structure without invoking geometric embedding or spatial coordinates.

While prior work has shown the computational difficulty of minimizing tetrahedra in convex polyhedra [3], the present approach, rather than aiming for minimality, characterizes the symbolic and combinatorial constraints required for enclosure and internal decomposition. A central strength of the framework presented in this study is that it leads naturally to Euler’s characteristic, one of the foundational invariants in polyhedral topology. The identity

$$V - E + F = 2$$

emerges not by assumption, but as a direct consequence of empirically derived symbolic constraints involving internal triangulation segments, gluing surfaces, and tetrahedral decompositions. The extended form

$$V - E + F = 2(T - N_i + S_i)$$

provides a deeper lens into the interaction between internal and external structure. Based on the empirical formulas presented in this document, it was shown that for valid genus-zero decompositions,

$$T - N_i + S_i = 1$$

which guarantees the recovery of the classical Euler result. The fact that a purely combinatorial, coordinate-free framework yields this topological invariant is not incidental; it reflects the framework’s internal consistency and structural legitimacy. Unlike abstract proofs that assume closure, this derivation is constructive: Euler’s characteristic *emerges* from accounting for internal tetrahedra and their gluing segments and shared triangular surfaces.

That said, while this model enforces strict symbolic coherence, it does not guarantee geometric embeddability in three-dimensional Euclidean space. Certain configurations, especially those near the maximal “flatness” threshold (i.e., where the number of triangulation segments approaches its upper bound for polyhedron of vertices  $V$ ), may pass all combinatorial checks but still fail to realize as actual 3D polyhedra. These are symbolic false positives: structurally valid according to the framework, but geometrically unrealizable, due to overlap, crowding, or angular conflict.

This is not a weakness, but rather a natural boundary of combinatorial reasoning. It marks the limits between *combinatorial sufficiency* and *geometric necessity*. By identifying such edge cases, the framework defines the outer envelope of feasible structures and offers a direction for further refinement.

Future versions of the method may incorporate geometric heuristics, such as convexity filters, vertex angle bounds, or planarity constraints, to help exclude non-realizable cases. Computational embedding algorithms or realizability tests (based on graph-theoretic results like Steinitz’s theorem) could complement the current symbolic system, bridging toward a hybrid topological–geometric model.

Additionally, and as previously mentioned, the method is currently limited to genus-zero polyhedra, and does not yet account for higher-genus or non-manifold forms. Internal decompositions assume non-intersecting tetrahedra formed strictly through external and internal triangulation segments, without edge bisections or face subdivisions. Despite these constraints, this exploratory framework presents a symbolic heuristic for reasoning about polyhedral structure. It offers a consistent, transparent method for exploring enclosure, triangulation, and internal volume using nothing but integer logic. In doing so, it could open a pathway toward new classifications of polyhedra, and perhaps even toward insights into deeper rules that govern 3D structure.

## Code availability

A reference implementation of the symbolic enclosure framework developed in this paper is provided in the R package `polyenclose`. The package implements the symbolic feasibility checks, external and internal bounds, and face-type enumeration procedures described throughout the paper. It computes *necessary combinatorial conditions only* and does not attempt geometric realization or construction.

The code is available at:

<https://github.com/MoustaphaItani/polyenclose>

## 10 Acknowledgments

The author has no formal mathematical training and, despite seeking guidance over fifteen years ago, did not receive the mentorship or institutional support needed to develop these ideas at the time. Mental health difficulties further complicated the ability to engage in collaborative research across unfamiliar disciplines, and financial constraints prevented access to supplementary education. The mathematical concepts, results, and proofs presented in this paper originate entirely from the author’s independent observations, drawings, and combinatorial reasoning, developed between his early teenage years and early twenties.

The author thanks Mr. Mohammad Chalhoub for providing programming support to produce the table of restricted integer partitions (prior to the author realizing the sequence had long been established), and Mr. Amr Tamimi for introducing him in earlier years to Excel, both contributions made many years ago. More recently, the author thanks Mr. Tiago Monteiro-Henriques and Ms. Hajar Assaad for briefly reviewing the manuscript, and Ms. Federica Manca and Ms. Anu Virtanen for assistance with illustrations.

## References

- [1] Sami Mezal Almohammad, Márton Naszódi, and Zsolt Lángi. An analogue of a theorem of steinitz for ball polyhedra in  $\mathbb{R}^3$ . arXiv:2011.10105, 2020. arXiv preprint.
- [2] George E. Andrews. *The Theory of Partitions*, volume 2 of *Encyclopedia of Mathematics and its Applications*. Addison-Wesley, Reading, MA, 1976.
- [3] Alexander Below, Jesús A De Loera, and Jürgen Richter-Gebert. The complexity of finding small triangulations of convex 3-polytopes. *Journal of Algorithms*, 50(2):134–167, 2004.
- [4] David Eppstein, John M. Sullivan, and Alper Üngör. Tiling space and slabs with acute tetrahedra. *Computational Geometry*, 27(3):237–255, 2004.
- [5] Jean Gallier and Jocelyn Quaintance. Aspects of convex geometry: Polyhedra, linear programming, shellings, voronoi diagrams, delaunay triangulations. Unpublished book manuscript / online draft, University of Pennsylvania, 2022. Available as an online PDF draft.
- [6] Branko Grünbaum. *Convex Polytopes*, volume 221 of *Graduate Texts in Mathematics*. Springer, New York, 2nd edition, 2003. See Chapter 13.
- [7] R. L. Naff. A control volume mixed finite element formulation for tetrahedral elements. *International Journal for Numerical Methods in Engineering*, 102(7):1400–1430, 2015. doi: 10.1002/nme.4820.
- [8] Ernst Steinitz. Polyeder und raumeinteilungen. In *Encyclopädie der mathematischen Wissenschaften*, volume 3-1-2, chapter 12, pages 1–139. B. G. Teubner, Leipzig, 1922.
- [9] Aman Timalcina and Matthew G. Knepley. Tetrahedralization of a hexahedral mesh. arXiv:2208.07128, 2022. arXiv preprint.
- [10] Günter M. Ziegler. Lectures on 0/1-polytopes. In Gil Kalai and Günter M. Ziegler, editors, *Polytopes – Combinatorics and Computation*, volume 29 of *DMV Seminar*, pages 1–41. Birkhäuser, 2000. Lecture Notes.

Supplementary Material for  
*Symbolic Constraints in Polyhedral Enclosure and Tetrahedral  
 Decomposition in Genus-0 Polyhedra*

Moustapha Itani

This document contains appendices and worked examples referenced in the main text.

## A Empirical Worked Examples ( $V = 4-7$ )

All results in this appendix are empirical examples obtained by manual construction. No general existence or completeness claim is made.

- $N$ : total surface angle units ( $180^\circ$  each)
- $S$ : external triangulation segments
- $F$ : faces;  $E$ : edges
- Face counts:  $F_k$  denotes the number of  $k$ -gonal faces ( $F_3$  triangles,  $F_4$  quadrilaterals,  $F_5$  pentagons,  $F_6$  hexagons)
- Vertex valencies:  $V_k$  denotes the number of vertices of degree  $k$  ( $V_3$  through  $V_6$ )
- $T$ : tetrahedra;  $N_i$ : internal gluing triangles;  $S_i$ : internal triangulation segments

Table 1: Empirical worked configurations for polyhedra with  $V = 4$  to  $V = 7$ . Each row represents a manually constructed example. The final two columns verify Euler's characteristic and the internal consistency relation  $T - N_i + S_i = 1$ .

$V$	$N$	$S$	$F$	$E$	$F_3$	$F_4$	$F_5$	$F_6$	$V_3$	$V_4$	$V_5$	$V_6$	$T$	$N_i$	$S_i$	$V-E+F$	$T-N_i+S_i$
4	4	0	4	6	4	-	-	-	4	-	-	-	1	0	0	2	1
5	6	0	6	9	6	0	-	-	2	3	-	-	2	1	0	2	1
		1	5	8	4	1	-	-	4	1	-	-	2	1	0	2	1
6	8	0	8	12	8	0	0	-	2	2	2	-	3	2	0	2	1
		0	8	12	8	0	0	-	0	6	0	-	4	4	1	2	1
		1	7	11	6	1	0	-	2	4	0	-	3	2	0	2	1
		1	7	11	6	1	0	-	3	2	1	-	3	2	0	2	1
		2	6	10	4	2	0	-	4	2	0	-	3	2	0	2	1
		2	6	10	5	0	1	-	5	0	1	-	3	2	0	2	1
7	10	0	10	15	10	0	0	0	2	3	0	2	4	3	0	2	1
		0	10	15	10	0	0	0	2	2	2	1	4	3	0	2	1
		0	10	15	10	0	0	0	1	3	3	0	5	5	1	2	1
		0	10	15	10	0	0	0	0	5	2	0	6	7	2	2	1
		1	9	14	8	1	0	0	3	2	1	1	4	3	0	2	1
		1	9	14	8	1	0	0	3	1	3	0	4	3	0	2	1
		1	9	14	8	1	0	0	2	3	2	0	4	3	0	2	1
		1	9	14	8	1	0	0	1	5	1	0	5	5	1	2	1
		2	8	13	7	0	1	0	3	3	1	0	4	3	0	2	1
		2	8	13	6	2	0	0	3	3	1	0	4	3	0	2	1
		3	7	12	6	0	0	1	6	0	0	1	4	3	0	2	1
		3	7	12	5	1	1	0	4	3	0	0	4	3	0	2	1
		3	7	12	4	3	0	0	4	3	0	0	4	3	0	2	1
4	6	11	3	2	1	0	6	1	0	0	4	3	0	2	1		

No claim is made that the listed configurations exhaust all admissible cases for the given vertex counts.

## B Topological Comparison of Tetrahedralization Strategies and Breakdown of the Proposed Identity with Internal Steiner Points

To evaluate how different tetrahedralization strategies affect the internal structure of a cube, I analyze key topological quantities including the number of tetrahedra  $T$ , internal gluing triangle faces  $N_i$ , and internal triangulation segments  $S_i$ . The proposed identity

$$T - N_i + S_i = 1$$

is observed to hold consistently across minimal and marching tetrahedra configurations, provided no internal vertices are added. However, once an internal Steiner point is introduced, particularly when it is treated as an internal vertex connected to new edges or faces, this relation fails. The following table presents a comparative breakdown of several configurations, highlighting how modeling assumptions (e.g., counting internal segments as edges or new pyramid faces as external) affect topological consistency. This analysis reinforces the significance of preserving external-only structure in minimal decompositions and offers a reference for evaluating topological soundness in more complex triangulations.

Table 2: Topological comparison of tetrahedralization strategies for a cube. The identity  $T - N_i + S_i = 1$  holds for decompositions without internal vertices, but fails once an internal Steiner point is introduced under various counting conventions.

Configuration	$V$	$E$	$F$	$T$	$N_i$	$S_i$	$E-F$	$2T-N_i$	$V-E+F$	$T-N_i+S_i$
Minimal	8	12	6	5	4	0	6	6	2	1
Marching tetrahedralization	8	12	6	6	6	1	6	6	2	1
Steiner not counted as vertex	8	12	6	12	18	0	6	6	2	-6
Steiner counted as vertex	9	12	6	12	18	0	6	6	3	-6
Steiner counted + edges	9	20	6	12	18	0	14	6	-5	-6
Steiner counted + edges + faces	9	20	18	12	6	0	2	18	7	6

This comparison demonstrates that the proposed identity is robust when internal structure arises solely from external constraints. In the minimal 5-tetrahedra decomposition, the identity holds exactly with no added internal triangulation segments. In the marching tetrahedralization strategy, although the identity still holds, the cube is bisected into two hexahedra by introducing an internal quadrilateral face. This increases internal complexity: one additional tetrahedron is required ( $T$  increases by 1), along with two new internal gluing triangles ( $N_i$ ) and one internal triangulation segment ( $S_i$ ). Nonetheless, the identity is preserved due to the balance between these added quantities. However, once a Steiner point is introduced inside the volume and treated as a vertex connected by new internal edges or faces, the identity fails. This breakdown reflects a fundamental shift in the topological model: the internal structure is no longer a consequence of surface triangulation alone, but instead includes additional volumetric elements. These results emphasize the importance of distinguishing between surface-conforming decompositions and those requiring internal augmentation when analyzing or designing tetrahedral meshes.

**Interpretation.** In the rows where interior faces/edges are counted together with boundary faces/edges, the quantity  $V - E + F$  is no longer the Euler characteristic of a 2-cell embedding of a closed surface. Rather, it is a mixed bookkeeping statistic for a 3-dimensional cell complex. Accordingly, values such as  $9 - 20 + 18 = 7$  do *not* indicate a failure of Euler's formula; they indicate that the counted  $(V, E, F)$  do not describe the boundary sphere alone. For the boundary 2-complex (faces only on  $\partial$ ), one still has  $V - E + F = 2$ . Now, compare with Appendix C for a case where invariance is preserved under surface-Steiner points.

## C Invariance of the Proposed Identity for Polyhedra with Surface-Embedded Edge Steiner Points

To illustrate the invariance of the identity  $T - N_i + S_i = 1$  under different tetrahedral decompositions, including those involving Steiner points, consider a single tetrahedron with one Steiner point placed on each

of three edges, each edge chosen such that the three Steiner points lie on the same face.

**Decomposition A (Plane Cut Through Three Steiner Points):**

Consider the plane passing through the three Steiner points. This plane divides the tetrahedron into two polyhedral regions:

- One region is a tetrahedron.
- The other is a five-faced polyhedron bounded by three quadrilateral faces and two triangular faces, with six vertices in total.

This five-faced polyhedron can be further decomposed into **three tetrahedra**, yielding a total of **four tetrahedra**. The tetrahedra are glued pairwise along **three internal triangular faces**, and the only Steiner points used are the original three placed on the edges.

Thus, the identity is satisfied:

$$T = 4, N_i = 3, S_i = 0 \Rightarrow T - N_i + S_i = 4 - 3 + 0 = 1$$

**Decomposition B (Edge-Based Slicing Through Steiner Points):**

Alternatively, one can sequentially slice the tetrahedron through one Steiner point at a time, joining each to the two original vertices that define its edge, and to one of the remaining original vertices, forming tetrahedra that share triangular faces. This approach also produces **four tetrahedra**, glued across the same number of internal triangular interfaces (**three**), and using the same **three Steiner points**.

Again, the identity holds:

$$T - N_i + S_i = 4 - 3 + 0 = 1$$

This example shows that **despite the different topology of the intermediate polyhedral shapes**, the identity is preserved, emphasizing its **combinatorial invariance** across Steiner-supported decompositions.

## D Worked Examples Demonstrating the Combinatorial Method for Testing 3D Polygonal Enclosure and Feasibility

This appendix presents worked examples that demonstrate the combinatorial method. It includes three examples that are combinatorially and geometrically valid, one example that is too flat to enclose, and an example of a likely false positive, a case where the set of polygons is determined symbolically valid but likely unrealizable.

### Worked Example: Four Triangles and One Quadrilateral (Square Pyramid)

- Step 1: Polygons: 1 square ( $P_4 = 1$ ), 4 triangles ( $P_3 = 4$ )
- Step 2:  $N = 6$
- Step 3:  $V = \frac{6}{2} + 2 = 5$
- Step 4:  $S = 1$
- Step 5:  $F = 5$
- Step 6:  $E = 3 \cdot (5 - 2) - 1 = 8$
- Step 7: Euler check:  $5 - 8 + 5 = 2$
- Step 8:  $S_{\text{ub}} = \frac{3}{2} \cdot 5 - \frac{13}{2} = 2$ ;  $S_{\text{difference}} = 1$  (passes flatness test)

### Worked Example: Six Squares (The Cube)

- Step 1: Polygons: 6 squares or quadrilaterals ( $P_4 = 6$ )
- Step 2:  $N = (4 - 2) \cdot 6 = 12$
- Step 3:  $V = \frac{12}{2} + 2 = 8$
- Step 4:  $S = (4 - 3) \cdot 6 = 6$
- Step 5:  $F = 6$
- Step 6:  $E = 3 \cdot (8 - 2) - 6 = 12$
- Step 7: Euler check:  $8 - 12 + 6 = 2$
- Step 8:  $S_{\text{ub}} = \frac{3}{2} \cdot 8 - 6 = 6$ ;  $S_{\text{difference}} = 0$  (passes flatness test)

### Worked Example: 12 Pentagons (The Dodecahedron)

- Step 1: Polygons: 12 pentagons ( $P_5 = 12$ )
- Step 2:  $N = (5 - 2) \cdot 12 = 36$
- Step 3:  $V = \frac{36}{2} + 2 = 20$
- Step 4:  $S = (5 - 3) \cdot 12 = 24$
- Step 5:  $F = 12$
- Step 6:  $E = 3 \cdot (20 - 2) - 24 = 30$
- Step 7: Euler check:  $20 - 30 + 12 = 2$
- Step 8:  $S_{\text{ub}} = \frac{3}{2} \cdot 20 - 6 = 24$ ;  $S_{\text{difference}} = 0$  (passes flatness test)

### Worked Example: 36 Hexagons

- Step 1: Polygons: 36 hexagons ( $P_6 = 36$ )
- Step 2:  $N = 144$
- Step 3:  $V = \frac{144}{2} + 2 = 74$
- Step 4:  $S = 108$
- Step 5:  $F = 36$
- Step 6:  $E = 3 \cdot (74 - 2) - 108 = 108$
- Step 7: Euler check:  $74 - 108 + 36 = 2$
- Step 8:  $S_{\text{ub}} = \frac{3}{2} \cdot 74 - 6 = 105$ ;  $S_{\text{difference}} = -3$  (fails flatness test)

**Conclusion:** A set of 36 hexagons cannot produce an enclosed polyhedron.

## Worked Example: Two Hexagons and Four Triangles (False Positive)

- **Step 1:** Polygons: 2 hexagons ( $P_6 = 2$ ), 4 triangles ( $P_3 = 4$ )
- **Step 2:**  $N = (6 - 2) \cdot 2 + (3 - 2) \cdot 4 = 8 + 4 = 12$
- **Step 3:**  $V = \frac{12}{2} + 2 = 8$
- **Step 4:**  $S = (6 - 3) \cdot 2 + (3 - 3) \cdot 4 = 6 + 0 = 6$
- **Step 5:**  $F = 6$
- **Step 6:**  $E = 3 \cdot (8 - 2) - 6 = 12$
- **Step 7:** Euler check:  $V - E + F = 8 - 12 + 6 = 2$  (passes)
- **Step 8:**  $S_{\text{ub}} = \frac{3}{2} \cdot 8 - 6 = 6$ ,  $S_{\text{difference}} = 0$  (passes flatness)

**Conclusion:** This configuration passes all combinatorial checks: Euler’s formula holds, edge and face counts are consistent, the triangulation segment count meets the flatness threshold, and a minimal internal tetrahedral decomposition is arithmetically feasible. However, no known convex or non-convex polyhedron with exactly two hexagons and four triangles exists in the literature. The structure cannot be embedded in  $\mathbb{R}^3$  as a genus-zero surface with non-self-intersecting faces. This mismatch illustrates the boundary between symbolic sufficiency and geometric feasibility. While the framework successfully captures algebraic consistency, it cannot, by design, account for spatial constraints such as embeddability or convex closure. This example thus serves as a clear case where realizability remains unresolved. No known convex or non-convex realization exists.

When substituting two of the triangles with one quadrilateral, keeping the total face count at six, the resulting configuration becomes *too flat* to enclose. This failure highlights how even minimal changes in polygonal composition can push a structure past the limits of combinatorial enclosure. Such sensitivity underscores the **brittleness** of symbolic tetrahedral enclosure near flatness thresholds. The substitution of two triangles with a quadrilateral may therefore serve as a practical diagnostic for testing the **combinatorial resilience** of enclosure candidates. Identifying and interpreting such tipping points offers a pathway for refining this framework and integrating embeddability heuristics in future work.

## E Numerical values of $\text{Combinations}_{\text{lb}}(V)$

Table 3: Lower-bound estimates of the number of admissible external–internal macro-configuration pairs,  $\text{Combinations}_{\text{lb}}(V)$ , as a function of vertex count  $V$ .

$V$	Estimated total configuration sets
4	1
5	2
6	5
7	8
8	13
9	18
10	25
11	32
12	41
13	50
14	61
15	72
16	85
17	98
18	113
19	128
20	145

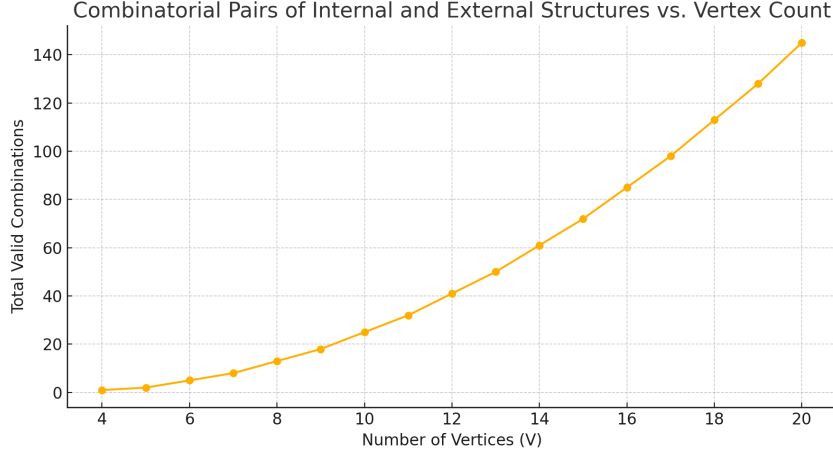


Figure 1: Combinatorial sum of internal and external structure groupings as a function of vertex count.

## F Combinatorial Identities and Bounds

This appendix records (i) *proved* external and topological identities used in the main text, and (ii) the *empirical/heuristic* identities and bounds collected from worked decompositions. All variables are symbolic and coordinate-free. Genus 0 and normal-form assumptions apply where stated. All linear “max” values quoted below are valid within the SALT+MIE class. Non-SALT triangulations can exceed these bounds.

### F.1 Proved External Identities and Bounds

Exact external formulas for genus-0 polyhedra in normal form:

$$E = 3V - 6 - S \tag{E.1}$$

$$F = 2V - 4 - S \tag{E.2}$$

where

$$S = \sum_f (\deg f - 3) \quad (\text{flatness, total deviation from triangulation}).$$

From the vertex degree constraint  $\deg(v) \geq 3$ , one obtains the sharp bounds:

Even  $V$ :

$$0 \leq S \leq \frac{3V}{2} - 6, \tag{E.3a}$$

$$\frac{3V}{2} \leq E \leq 3V - 6, \tag{E.4aE}$$

$$\frac{V}{2} + 2 \leq F \leq 2V - 4. \tag{E.4aF}$$

Odd  $V$ :

$$0 \leq S \leq \frac{3V}{2} - \frac{13}{2} \tag{E.3b}$$

$$\frac{3V+1}{2} \leq E \leq 3V - 6 \tag{E.4bE}$$

$$\frac{V}{2} + \frac{5}{2} \leq F \leq 2V - 4 \tag{E.4bF}$$

**Extremal Values Summary (genus-0, normal form)**

$V$ parity	$S_{\text{ub}}$	$E_{\text{lb}}$	$E_{\text{ub}}$	$F_{\text{lb}}$	$F_{\text{ub}}$
Even $V$	$\frac{3V}{2} - 6$	$\frac{3V}{2}$	$3V - 6$	$\frac{V}{2} + 2$	$2V - 4$
Odd $V$	$\frac{3V}{2} - \frac{13}{2}$	$\frac{3V+1}{2}$	$3V - 6$	$\frac{V}{2} + \frac{5}{2}$	$2V - 4$

Angle-unit bookkeeping (fully triangulated boundary):

$$F_{\Delta} = F + S = 2V - 4 \quad (\text{E.5})$$

$$F_{\Delta} = 4T - 2N_i \quad (\text{E.6})$$

(Equation (E.6) counts triangle units: each tetrahedron contributes 4, each internal gluing triangle cancels 2.)

## F.2 Proved Topological Identity for 3D Complexes

For any tetrahedralization of a 3-ball (genus-0 volume) with  $V_i$  interior vertices and  $E_i$  interior edges,

$$T - N_i + E_i - V_i = 1 \quad (\text{E.7})$$

(Prop. ??). In particular, when  $V_i = 0$  (normal form, no interior vertices),

$$T - N_i + E_i = 1. \quad (\text{E.8})$$

## F.3 Bridge to the Heuristic Extended Euler Form

A heuristic identity used in the text is

$$V - E + F = 2(T - N_i + S_i) \quad (\text{E.9h})$$

and the SALT ladder case asserts

$$T - N_i + S_i = 1. \quad (\text{E.10h})$$

**Convention (SALT+MIE).** In the SALT+MIE setting we identify  $S_i$  with the interior-edge count  $E_i$ ; outside SALT+MIE,  $S_i$  denotes the number of interior triangulation segments used in the chosen refinement and need not coincide with  $E_i$ .

These coincide with (E.7)–(E.8) whenever  $V_i = 0$  and  $S_i = E_i$  (as in SALT+MIE constructions).

## F.4 Core Equations (proved unless marked heuristic)

$$\text{(E.9h)} \quad V - E + F = 2(T - N_i + S_i) \quad (\text{heuristic}) \quad (1)$$

$$\text{(E.10h)} \quad T - N_i + S_i = 1 \quad (\text{SALT ladder case}) \quad (2)$$

$$\text{(E.11r)} \quad N_i = 2T - V + 2 \quad (\text{exact in normal form; no interior vertices}) \quad (3)$$

$$\text{(E.12r)} \quad E - F = 2T - N_i \quad (\text{from (E.1)–(E.2) + Euler}) \quad (4)$$

## F.5 Restricted SALT+MIE ranges (heuristic / construction-based)

$$\text{(E.13r)} \quad T_{\min} = V - 3 \quad (5)$$

$$\text{(E.14r)} \quad T_{\max} = 2(V - 4) \quad (6)$$

$$\text{(E.15r)} \quad N_{i,\min} = V - 4 \quad (7)$$

$$\text{(E.16r)} \quad N_{i,\max} = 3(V - 4) - 2 \quad (8)$$

## F.6 Derived Relationships (algebraic within SALT+MIE)

The following are algebraic consequences of (E.13r)–(E.16r); they are not independent results.

$$(E.17r) \quad T_{\max} = 2N_{i,\min} \quad (9)$$

$$(E.18r) \quad N_{i,\max} = \frac{3}{2}T_{\max} - 2 \quad (10)$$

$$(E.19r) \quad N_{i,\max} = 2N_{i,\min} + (V - 6) \quad (11)$$

$$(E.20r) \quad N_{i,\max} - T_{\max} = N_{i,\min} - 2 \quad (12)$$

$$(E.21r) \quad N_{i,\max} - T_{\max} = T_{\min} - 3 \quad (13)$$

$$(E.22r) \quad N_{i,\min} = T_{\min} - 1 \quad (14)$$

$$(E.23r) \quad 2N_{i,\max} - 2T_{\max} = N_{i,\min} + T_{\min} - 5 \quad (15)$$

*Scope note.* Equations (E.1)–(E.8) are exact and universal topological identities. Equations (E.9h)–(E.23r) hold only heuristically or within the restricted SALT+MIE construction class.